Supporting Information for

Biochemical and Functional Evaluation of the Intramolecular Disulfide Bonds in the Zinc-Chelating Antimicrobial Protein Human S100A7 (Psoriasin)

Lisa S. Cunden,[1] Megan Brunjes Brophy,[1] Grayson E. Rodriguez,[1] Hope A. Flaxman,[1] and Elizabeth M. Nolan[1,*]

[1]Department of Chemistry, Massachusetts Institute of Technology, Cambridge, MA 02139, United States

*Corresponding author: lnolan@mit.edu

Phone: 617-452-2495

This Supporting Information includes:

Design of the synthetic genes for S100A7 variants…….. S4

Experimental Section……..…… S6

Materials and General Methods……..... S6

Purification of $S100A7_{red}$, $S100A7_{ox}$ and Variants…….. S9

Thioredoxin Activity Assays…… S10

Midpoint Potential (E_m) Determination…….. S11

Nernst Equation Derivation……..... S12

Logistic Equation Derivation…..…… S13

Reduction of $S100A7_{ox}$ by DTT, GSH, and TCEP…….. S14

Zn(II) Competition Titrations with S100A7 and Zincon…….. S14

Zinc Competition Assays with S100A7 and FZ3…… S14

Zinc Competition Titrations with S100A7 and ZP4 …… S15

Co(II) Binding Titrations and Metal Substitution Assays……..…… S15

Metal Analysis (ICP-MS)…….. S16

Antibacterial Activity Assays ……..…..……..…….. S17

Supporting Tables……..... S18

Table S1. Extinction coefficients for S100A7 variants.……..... S18

Table S2. Metal analysis (ICP-MS) of S100A7 from representative protein purifications…… S18

Table S3. Analytical SEC elution volumes and corresponding molecular weights for S100A7 variants…..……..……..……..…….. S19

Table S4. Fits for apparent $K_{d,Zn}$ values from ZP4 competition **t**itrations with S100A7 variants……..….. S19

Tables S5-S20. Metal depletion profiles of TSB :Tris medium treated with $S100A7_{ox}$, S100A7-Ser, and S100A7-Ala……..……..…….. S20

Table S21. List of strains and growth conditions employed in this work…… S25

Supporting Figures…… S26

Figure S1. Analytical HPLC traces for the purification of $S100A7\Delta_{ox}$…….. S26

Figure S2. SDS-PAGE of purified S100A7 variants……..…… S27

Figure S3. Analytical HPLC traces of S100A7 variants……..…..…… S28

Figure S4. CD spectra of S100A7 variants……..…. S29

Figure S5. Analytical SEC chromatograms of S100A7 variants…….. S30
Figure S6. Analytical HPLC traces of no enzyme controls for Trx/TrxR assays……. S31
Figure S7. Analytical HPLC traces showing air oxidation of $S100A7_{red}$…….. S31
Figure S8. Analytical HPLC traces of Ca(II) controls for Trx/TrxR assays..…….. S32
Figure S9. Analytical HPLC traces of Zn(II) controls for Trx/TrxR assays…….. S33
Figure S10. Equilibration times of $S100A7_{ox}$ for E_m determination…… S34
Figure S11. Analytical HPLC traces of S100A7 speciation for E_m determination……. S34
Figure S12. E_m determination using the Nernst and logistic functions…… S35
Figure S13. Analytical HPLC traces showing the reduction of apo vs. Zn(II)-bound $S100A7_{ox}$ by GSH, DTT and TCEP…… S36
Figure S14. Zincon competition titrations performed in the presence of Ca(II)……. S37
Figure S15. ZP4 competition fits of $S100A7_{ox}$…….. S38
Figure S16. ZP4 competition fits of $S100A7_{red}$…… S39
Figure S17. ZP4 competition fits of S100A7-Ser…… S40
Figure S18. ZP4 competition fits of S100A7-Ala……. S41
Figure S19. Simulations of fits for S100A7 variants competition with ZP4……. S42
Figure S20. Metal analysis of Tris:TSB medium treated with S100A variants…….. S43
Figure S21. Analytical HPLC traces showing S100A7 speciation following incubation in Tris:TSB medium……. S44
Figure S22. CFU assay with *E. coli* ATCC 25922 and K-12 with $S100A7_{ox}$…..…….. S45
Figure S23. Co(II)-binding titrations with S100A7-Ser and S100A7-Ala……. S45
Figure S24. Co(II)-binding titrations of S100A7 variants in the presence of Ca(II)….. S46
Supporting References……. S47

Design of the Synthetic Genes for Human S100A7 Variants

The synthetic gene for human S100A7 was previously described.[1] Briefly, it was optimized for *E. coli* codon usage and ordered from DNA 2.0. A *Nde*I restriction site was placed at the 5' end. A stop codon and a *Xho*I restriction site were placed at the 3' end. This gene was received in the pJ201 vector from DNA 2.0. The gene was sub-cloned into the *Nde*I and *Xho*I sites of pET41a to afford pET41a-*S100A7* for protein expression. Synthetic genes were designed in the same manner for the variants S100A7-Ser, S100A17-Ala, and S100A7ΔHis$_3$Asp. The *E. coli* optimized genes were sub-cloned into the *Nde*I and *Xho*I sites of pET41a.

1. For the S100A7-Ser variant

***E. coli* optimized nucleotide sequence for NdeI-**S100A7(C47S)(C96S)-Stop**-XhoI:**
CATATGAGCAACACCCAGGCAGAACGTAGCATTATTGGTATGATTGACATGTTTCACAAATA
CACGCGTCGCGATGACAAAATCGATAAGCCGAGCCTGTTGACCATGATGAAAGAGAACTTT
CCGAATTTTCTGAGCGCGTCTGATAAGAAGGGTACGAACTACCTGGCTGATGTTTTCGAGA
AGAAAGACAAGAATGAGGATAAGAAAATCGACTTCTCGGAATTCCTGAGCCTGCTGGGCG
ACATCGCGACCGACTATCATAAACAGAGCCACGGCGCAGCCCCGTCCAGCGGTGGTAGC
CAA**TAA**CTCGAG

Translated sequence for NdeI-S100A7(C47S)(C96S)-Stop**-XhoI:**
MSNTQAERSI IGMIDMFHKY TRRDDKIDKP SLLTMMKENF PNFLSASDKK GTNYLADVFE
KKDKNEDKKI DFSEFLSLLG DIATDYHKQS HGAAPSSGGS Q Stop **L E**

2. For the S100A7-Ala variant

***E. coli* optimized nucleotide sequence for NdeI-**S100A7(C47A)(C96A)-Stop**-XhoI:**
CATATGAGCAACACCCAGGCAGAACGTAGCATTATTGGTATGATTGACATGTTTCACAAATA
CACGCGTCGCGATGACAAAATCGATAAGCCGAGCCTGTTGACCATGATGAAAGAGAACTTT
CCGAATTTTCTGAGCGCGGCGGATAAGAAGGGTACGAACTACCTGGCTGATGTTTTCGAG
AAGAAAGACAAGAATGAGGATAAGAAAATCGACTTCTCGGAATTCCTGAGCCTGCTGGGC
GACATCGCGACCGACTATCATAAACAGAGCCACGGCGCAGCCCCGGCGAGCGGTGGTAG
CCAA**TAA**CTCGAG

Translated sequence for NdeI-S100A7(C47A)(C96A)-Stop**-XhoI:**
MSNTQAERSI IGMIDMFHKY TRRDDKIDKP SLLTMMKENF PNFLSAADKK GTNYLADVFE
KKDKNEDKKI DFSEFLSLLG DIATDYHKQS HGAAPASGGS Q Stop **L E**

3. For the S100A7 ΔHis$_3$Asp variant

***E. coli* optimized nucleotide sequence for NdeI-**S100A7(H18A)(D25A)(H87A)(H91A)-Stop**-XhoI:**
CATATGAGCAACACCCAGGCAGAACGTTCCATTATTGGTATGATTGATATGTTTGCGAAATA
CACCCGCCGTGACGCCAAGATCGATAAACCGAGCTTGCTGACGATGATGAAAGAGAACTT
CCCGAATTTCCTGTCGGCTTGTGATAAGAAGGGCACGAACTATCTGGCAGACGTTTTCGAG
AAGAAAGACAAAAATGAGGATAAGAAGATCGACTTTAGCGAATTTCTGAGCCTGCTGGGTG
ATATCGCGACCGACTACGCGAAACAGAGCGCCGGTGCGGCACCGTGCAGCGGCGGTTCT
CAA**TAA**CTCGAG

Translated sequence for NdeI- S100A7(H18A)(D25A)(H87A)(H91A)-Stop**-XhoI:**
MSNTQAERSI IGMIDMFAKY TRRDAKIDKP SLLTMMKENF PNFLSACDKK GTNYLADVFE KKDKNEDKKI DFSEFLSLLG DIATDYAKQS AGAAPCSGGS Q Stop **L E**

For the nucleotide sequence, the restriction sites and stop codon are underlined and in bold, respectively.

For the amino acid sequence, the mutated residues are highlighted in yellow.

Experimental Section

Materials and General Methods. All solvents and chemicals were obtained from commercial suppliers as detailed below and used as received. All aqueous solutions were prepared using Milli-Q water (18.2 MΩ•cm, 0.22-μm filter). Protein concentrations were routinely quantified by using the calculated extinction coefficients for the S100A7 homodimer (ProtParam: ε_{280} = 9190 $M^{-1}cm^{-1}$ for $S100A7_{ox}$ and $S100A7\Delta_{ox}$; ε_{280} = 8940 $M^{-1}cm^{1}$ for $S100A7_{red}$, S100A7-Ser, S100A7-Ala, and $S100A7\Delta_{red}$; Table S1 includes ε_{280} values for the S100A7 monomers). All protein concentrations are for the S100A7 homodimer, and all reported stoichiometries are relative to the S100A7 homodimer.

Commercial materials, buffers, and solution preparations. Human thioredoxin (Sigma-Aldrich and Fisher Scientific) and rat liver thioredoxin reductase (Sigma-Aldrich) were stored according to manufacturer protocols, and used as received. NADPH reduced form tetrasodium salt was obtained from Tocris Bioscience; GSH from Sigma-Aldrich; GSSG from Alfa Aesar; guanidinium hydrochloride (GuHCl) from Sigma-Aldrich. Solutions of GuHCl were filtered through a 0.22-μm millipax filter and stored in glass bottles. Chelex resin was purchased from Bio-Rad.

For metal-binding experiments and redox studies, metal-binding buffer (75 mM HEPES, 100 mM NaCl, pH 7.0) was prepared with Ultrol grade HEPES (free acid, Calbiochem) and TraceSELECT NaCl (Sigma), and TraceSELECT aqueous NaOH (Sigma) was used to adjust the solution pH. To reduce metal-ion contamination, plastic spatulas were used to transfer buffer reagents. A Tris buffer (1 mM Tris-HCl, pH 7.5) prepared from Tris base (J. T. Baker) was used for circular dichroism (CD) spectroscopy experiments. For experiments requiring anaerobic conditions, the buffers were degassed for at least 1 h by Ar bubbling, and then transferred to an anaerobic glovebox (Vac Atmospheres, N_2 atmosphere) where they were equilibrated for at least 24 h before an experiment and subsequently stored in the glovebox.

Stock solutions of $CoCl_2$ (100 mM, 100 mL), $CaCl_2$ (1 M, 100 mL), and $ZnCl_2$ (100 mM,

100 mL) were prepared from 99.999% $CoCl_2$ (Sigma), $CaCl_2$ (Sigma), and $ZnCl_2$ (Sigma, anhydrous) respectively, and Milli-Q water. The metal stock solutions were prepared in acid-washed volumetric glassware and transferred to sterile polypropylene tubes for long-term storage. The working solutions were prepared by diluting the stock solutions in Milli-Q water.

For Zn(II) competition experiments, the competitors Zincon monosodium salt (Sigma-Aldrich), FluoZin-3 (FZ3, Fisher Scientific), and Zinpyr-4 (ZP4, Strem Chemicals) were employed. Stock solutions (≈10 mM) of Zincon and ZP4 (≈2 mM) were prepared in anhydrous DMSO (Sigma), aliquoted into 50-μL portions, and stored at -20 ^{o}C. Stocks of FZ3 (≈2 mM) were prepared in Milli-Q water, aliquoted into 10-μL portions, and stored at -20 ^{o}C. Each aliquot was thawed only once, and experiments with these reagents were performed in the dark.

For the metal-depletion experiments and antibacterial activity assays, Tryptic Soy Broth (TSB) medium (Becton Dickinson), deMan, Rogosa, and Sharpe (MRS) medium (Becton Dickinson), and Brain Heart Infusion (BHI) medium (Becton Dickinson) were prepared with Milli-Q water.

$HD5_{ox}$ preparation and handling. $HD5_{ox}$ was prepared and stored as described in the literature.[2] The calculated extinction coefficient of ε_{278} = 3181 $M^{-1}cm^{-1}$ for $HD5_{ox}$ was employed to determine peptide concentration.

Optical Absorption and Fluorescence Spectroscopy. Optical absorption spectra were collected on a Beckman Coulter DU 800 spectrophotometer thermostatted at 25 °C with a Peltier temperature controller. Quartz cuvettes with 1-cm path lengths (Starna) were employed for all optical absorption measurements. Fluorescence spectra were collected on a Photon Technologies International QuantaMaster 40 fluorimeter outfitted with a continuous xenon source for excitation, autocalibrated QuadraScopic monochromators, a multimode PMT detector, and a circulating water bath maintained at 25 °C. This instrument was controlled by the FelixGX

software package. Either quartz (Starna) or PMMA (Fischer Scientific) cuvettes with 1-cm path lengths were employed for fluorescence measurements.

CD Spectroscopy. An Aviv Model 202 CD spectrometer was employed to collect CD spectra. Protein was buffer exchanged into 1 mM Tris-HCl, pH 7.5 and then transferred (10 μM, 300 μL) and transferred to a Hellma quartz cuvette (1-mm path length). The CD spectra were recorded from 195 to 260 nm at 1-nm intervals. Each measurement was averaged for 3 sec, and three independent scans were conducted. The averaged data are reported.

Analytical HPLC. Analytical HPLC was performed on an Agilent 1200 instrument equipped with a thermostatted autosampler set at 4 °C, a thermostatted column compartment set at 20 °C, and a multi-wavelength detector set at 220 and 280 nm (500 nm reference wavelength, 100 nm bandwidth). A Proto C4 column (5-μm pore, 4.6 x 250 mm, Higgins Analytical Inc.) and a flow rate of 1 mL/min with a gradient of 35–50% B over 30 min was employed for all analytical HPLC experiments with S100A7. A Clipeus C18 column (5-μm pore, 4.6 x 250 mm, Higgins, Inc.) and a flow rate of 1 mL/min with a gradient of 10–60% B over 25 min was employed all analytical HPLC experiments with $HD5_{ox}$.. For all analytical HPLC, solvent A was 0.1% TFA/H_2O and solvent B was 0.1% TFA/MeCN.

LC-MS. An Agilent 1290 series LC system equipped with an Agilent 6230 TOF system housing Agilent Jetstream ESI source was employed to perform high-resolution mass spectrometry. An Agilent Poroshell 300SB-C18 column (5-μm pore) was employed. Solvent A was 0.1% formic acid/H_2O. Solvent B was 0.1% formic acid/MeCN. Protein samples (10 μM) were prepared in Milli-Q water and 1 μL was injected for each analysis. Data was acquired by using the Agilent MassHunter Workstation Data Acquisition software and processed with the Agilent MassHunter Qualitative Analysis program. All ESI-MS spectra were acquired in positive ion mode.

Analytical SEC. Analytical SEC was conducted using an ÄKTA purification system with a Superdex 75 10/300 GL column (GE Healthcare Life Sciences) housed at 4 °C as previously described.[1]

Purification of Human S100A7$_{red}$, S100A7$_{ox}$ and Variants. The synthetic gene for human S100A7 and the pET-41a-*S100A7* vector were previously described.[1] The synthetic genes containing the *E. coli* optimized nucleotide sequence for human S100A7-Ala, S100A7-Ser, and S100A7Δ were sub-cloned into the *Nde*I and *Xho*I sites of pET41a by DNA 2.0. The identity of each plasmid was confirmed by DNA sequencing (MIT Biopolymers or Quintarabio). Each S100A7 protein was overexpressed in *E. coli* BL21(DE3) as previously described for human S100A7.[1] S100A7-Ser and S100A7-Ala were purified and stored using the original protocol reported for S100A7.[1] To obtain S100A7$_{red}$ and S100A7$_{ox}$, as well as S100A7Δ$_{red}$ and S100A7Δ$_{ox}$, the original purification protocol was also followed,[1] and additional steps were performed after the SEC step to fully reduce or fully oxidize the protein. In general, the protein purifications for the S100A7 variants were carried out starting from 2 L of *E. coli* cell culture.

For the purification of S100A7$_{red}$ and S100A7Δ$_{red}$ from a 2-L culture, after the SEC step (75 mM HEPES, 100 mM NaCl, pH 7.0, or 20 mM Tris, 100 mM NaCl, pH 7.5), fractions containing S100A7 were pooled and transferred to a Spectropor3 3500 MWCO dialysis bag. The protein was dialyzed against 1 L of 75 mM HEPES, 1 mM DTT, 100 mM NaCl, pH 7.0 containing ≈10 g Chelex resin at 4 ^{o}C for ≈12 h. The dialysate was passed through a 0.45-μm syringe filter to remove any contaminating Chelex resin. The protein was concentrated using an Amicon 10-kDa MWCO spin filter (3750 rpm, 4 ^{o}C) to >500 μM, partitioned into sterile microcentrifuge tubes in 50-μL aliquots, flash frozen in liquid nitrogen, and stored at -80 ^{o}C.

For the purification of S100A7$_{ox}$ and S100A7Δ$_{ox}$, the original S100A7 purification protocol was followed except that the SEC was performed using a Tris running buffer (20 mM Tris, 100 mM NaCl, pH 7.5). Fractions containing S100A7 were pooled and diluted to 20 μM in 20 mM Tris, 100 mM NaCl, pH 7.5, and the solution was transferred to a 150-mL glass beaker. For the

Cu(II)-catalyzed oxidation of $S100A7_{ox}$, three equivalents of Cu(II) (≈90 μL from a 100-mM stock solution of $CuCl_2$) were added dropwise to the protein solution and the mixture was incubated at room temperature for 2 h with stirring. The oxidation state of the protein was confirmed by HPLC analysis. For the Cu(II)-catalyzed oxidation of S100A7Δ, two equivalents of Cu(II) (≈60 μL from a 100-mM stock solution of $CuCl_2$) were added dropwise to the protein solution, and the mixture was incubated at room temperature for 2 h with stirring. A precipitate formed, and the mixture was centrifuged (3750 rpm, 10 min, 4 ^{o}C) to remove the precipitate. The resulting solution containing soluble protein and copper was incubated overnight with stirring at room temperature. The oxidation state of the protein was confirmed by HPLC analysis. The resulting protein solution ($S100A7_{ox}$ or $S100A7\Delta_{ox}$) was then transferred to a Spectropor3 3500 MWCO dialysis bag and dialyzed overnight against 1 L of 75 mM HEPES, 100 mM NaCl, pH 7.0 containing ≈10 g Chelex resin (Biorad), and 1 mM EDTA at 4 ^{o}C. The EDTA was subsequently removed by dialysis against 75 mM HEPES, 100 mM NaCl, pH 7.0 (2 x 4 L, ≈12 h per dialysis, 4 ^{o}C). The protein was then concentrated using an Amicon 10-kDa MWCO spin filter (3750 rpm, 4 ^{o}C) to >500 μM, partitioned into sterile microcentrifuge tubes in 50-μL aliquots, flash frozen in liquid nitrogen, and stored at -80 ^{o}C. The metal contents of the purified oxidized proteins were analyzed by ICP-MS and were found to contain ≈0.03 and ≈0.04 equivalents of Cu and Zn, respectively (Table S2).

These procedures afforded protein yields that ranged from ≈30-80 mg/L of cell culture. In general the yields were 50-80 mg/L of S100A7-Ser and S100A7-Ala, and 30-50 mg/L of $S100A7_{ox}$, $S100A7_{red}$, $S100A7\Delta_{ox}$, and S100A7 Δ_{red}. Protein aliquots were freeze-thawed only once. All experiments were performed with at least two independent batches of purified proteins. Tables S1-S3 and Figures S2-S5 detail the purity, identity, and basic biochemical characterization of these proteins.

Thioredoxin Activity Assays. Solutions (500 μL) containing 5 μM $S100A7_{ox}$, 1 μM human thioredoxin (Trx), 100 nM rat liver thioredoxin reductase (TrxR), and 1 mM NADPH in 75

mM HEPES, 100 mM NaCl, pH 7.0, were prepared and incubated at 37 ^{o}C. To initiate the reaction, Trx was added last. A 100-μL aliquot was collected at each time point (t = 0, 15 and 120 min), immediately quenched with 10 μL of 6% TFA, followed by the addition of 50 μL of 6 M GuHCl. The quenched samples were centrifuged (13 000 rpm x 5 min, 4 °C), and the resulting supernatants (120 μL aliquot) analyzed by HPLC. To investigate the effect of Ca(II) on the reduction of $S100A7_{ox}$ by Trx/TrxR, these experiments were also performed in the presence of 2 mM Ca(II). To investigate the effect of Zn(II) on the reduction of $S100A7_{ox}$ by Trx/TrxR, Zn(II) (1.9 equiv) was added to $S100A7_{ox}$, and the sample was incubated for at least 15 min prior to the start of the experiment. This Zn(II):S100A7 homodimer ratio was used to minimize the amount of unbound Zn(II) in the assay because Zn(II) inhibits the activity of Trx/TrxR.[3] Following optimization, each experiment was performed in duplicate and HPLC traces from one experiment are presented.

The peptide $HD5_{ox}$, which we study in an independent initiative, binds neither Ca(II) nor Zn(II) and is a substrate for Trx/TrxR.[4] We used Trx/TrxR-catalyzed reduction of $HD5_{ox}$ to $HD5_{red}$ in control assays to confirm that the presence of Ca(II) or Zn(II)-bound $S100A7_{ox}$ did not cause enzyme inhibition. In a first set of assays, $HD5_{ox}$ reduction in the absence and presence of 2 mM Ca(II) was monitored over time (t = 0, 5, 10, 15 and 120 min). This assay was conducted as described above using 10 μM $HD5_{ox}$. In a second set of assays, $HD5_{ox}$ was co-incubated with Zn(II)-bound $S100A7_{ox}$, and $HD5_{ox}$ reduction by Trx/TrxR was monitored over time (t = 0, 5, 10, 15 and 120 min). This assay was conducted as described above for the Zn(II):$S100A7_{ox}$ experiment except that 10 μM $HD5_{ox}$ was included in the assay mixture.

Midpoint Potential (E_m) Determination. These experiments were designed based on a reported procedure.[4] All redox buffers were prepared at room temperature in a glovebox, and the assays were performed in a glovebox. In order to prepare buffers of defined redox potentials, aqueous stock solutions of GSH and GSSG (10 mL, 10 mM) were prepared in the glovebox using volumetric flasks (75 mM HEPES, 100 mM NaCl, pH 7.0, ± 2mM Ca(II)). Using these

solutions, buffers with redox potentials spanning the -200 to -400 mV range were prepared in ≈7-mV increments using GSH and GSSG ratios determined by the Nernst equation (75 mM HEPES, 100 mM NaCl, pH 7.0, ± 2 mM Ca(II)). The midpoint potential (E_m) of S100A7 was determined by incubating $S100A7_{ox}$ (10 μM) in each redox buffer under anaerobic conditions at 37 °C. For the experiments with apo $S100A7_{ox}$, solutions of $S100A17_{ox}$ (10 μM, 200 μL) were prepared in the appropriate redox buffers (-200 to -400 mV). The samples were prepared in a 96-well plate with each well containing a sample at a specified redox value. For experiments performed in the presence of 2 mM Ca(II), the samples were prepared by the same procedure except that the buffer contained 2 mM Ca(II). The plate was sealed, and incubated in a heat block at 37 °C anaerobically for ≈96 h (4 days). Then, the samples were quenched with 10 μL of 6% aqueous TFA. The quenched samples were removed from the glovebox, transferred to microcentrifuge tubes, and centrifuged (13 000 rpm x 5 min, 4 °C). The resulting supernatants (120 μL aliquot) were analyzed by HPLC. The redox potential of the S100A7 disulfide bond was determined from the equilibrium between $S100A7_{ox}$ and $S100A7_{red}$ as quantified by HPLC (integration of peak areas). The E_m values were first estimated from the data plotted in Figure 4 by determining the midpoint potential value that provides a 1:1 ratio of $S100A7_{ox}$ and $S100A7_{red}$. We did not include the S100A7-glutathione disulfide adduct that formed (≈15.9 min retention time, Figure S11) in the calculation because this equilibrium is independent of the equilibrium between $S100A7_{ox}$ and $S100A7_{red}$. We did not perform experiments starting from $S100A7_{red}$ because, during trial assays, we observed marked formation of the protein-glutathione adduct that accounted for up to 30% of the total protein and did not obtain reproducible results. Each experiment was performed at least three times, and errors are shown at SDM.

Nernst Equation Derivation. The midpoint potential (E_m) of S100A7 was determined by incubating $S100A7_{ox}$ in buffers at defined redox potentials prepared using the reduced (GSH) and oxidized (GSSG) forms of glutathione as described above. The [GSH] / [GSSG] ratio needed for a specified redox potential value was calculated using the Nernst equation as follows:

$$E_{buffer} = E^{o}_{m\,(GSH/GSSG)} - \frac{RT}{nF}\ln\left(\frac{[GSH]^2}{[GSSG]}\right) \quad \text{(eq. 1)}$$

where $E^{o}_{m\,(GSH/GSSG)}$ is the midpoint potential of the glutathione redox couple, R is the universal gas constant (8.314 $JK^{-1}mol^{-1}$), T is the temperature (310.2 K), *n* is the number of moles of electrons transferred (2 electrons per disulfide bond; *n* = 2 for glutathione and *n* = 2 per monomer of S100A7), and F is the Faraday constant (9.6485 x 10^4 $Cmol^{-1}$). At pH 7.0, $E^{o}_{m\,(GSH/GSSG)}$ is -240 mV.[5] Therefore, eq. 1 can be rewritten as follows:

$$E_{buffer} = -240\ mV - \frac{61.5}{2}\log\left(\frac{[GSH]^2}{[GSSG]}\right) \quad \text{(eq. 2)}$$

Attempts to obtain E_m values of S100A7 in the absence and presence of Ca(II) by fitting the data to the Nernst Equation (eq. 3) resulted in poor fits as discussed in the main text.

$$E^{o}_{m\,(S100A7red/S100A7ox)} - \left(\frac{61.5}{2}\right)\log\left(\frac{S100A7_{red}}{S100A7_{ox}}\right) = -240\ mV - \frac{61.5}{2}\log\left(\frac{[GSH]^2}{[GSSG]}\right) \quad \text{(eq. 3)}$$

Logistic Equation Derivation. Data fitting showed that the midpoint data was not well fit using the Nernst equation because conversion to 100% of $S100A7_{ox}$ could not be reached under the experimental conditions. We therefore employed a logistic function (eq. 4) and allowed the calculated maxima to vary during data fitting, which provided better fits for the midpoint potential determination of $S100A7_{ox}$.

$$F(x) = \%S100A7_{ox-max}/(1 + \exp(-k * (E_{buffer} - E^{o}_{m\,(S100A7red/S100A7ox)}))) \quad \text{(eq. 4)}$$

where *F(x)* is percentage of $S100A7_{ox}$ at a specified redox potential value (E_{buffer}), $\%S100A7_{ox-max}$ is the maximum percentage of $S100A7_{ox}$ obtained, *k* is a variable that accounts for temperature, the universal gas constant, Faraday's constant, and moles of electrons

transferred, and $E^{o}_{m\,(S100A7red/S100A7ox)}$ is the midpoint potential of S100A7.

Reduction of S100A7$_{ox}$ by DTT, GSH, and TCEP. A 400-μL sample containing 30 μM of S100A7$_{ox}$ (75 mM HEPES, 100 mM NaCl, pH 7.0) was allowed to incubate at room temperature in the presence of 1 mM DTT, GSH, or TCEP (4 μL from a 100-mM stock solution). A 45-μL aliquot was collected at each time point (t = 0, 5, 10, 15, 30, 60, and 120 min) and quenched with a mixture of 5 μL of 6% TFA and 100 μL of 6 M GuHCl. The quenched samples were centrifuged (13 000 rpm x 5 min, 4 °C), and the resulting supernatants (120 μL) were analyzed by HPLC. For samples containing Zn(II), the protein was incubated with 2 equivalents of Zn(II) for 15 min at room temperature prior to the addition of the reducing agent.

Zinc Competition Titrations with S100A7 and Zincon. A 2-mL solution containing S100A7 (10 μM) and Zincon (20 μM) was prepared in a quartz cuvette (75 mM HEPES, 100 mM NaCl, pH 7.0, ± 2 mM Ca(II)). The sample was titrated with Zn(II) in 2.5 μM increments up to 50 μM (1 μL from a 5-mM Zn(II) stock solution per addition). The sample was equilibrated for 2 min before the optical absorption spectrum was collected. For the titration with S100A7$_{red}$, the thawed protein sample was immediately buffer-exchanged to remove contaminating DTT (3 x 5 min, 13 000 rpm), mixed with Zincon, and Zn(II) titrated in. We observed no air-oxidation of S100A7$_{red}$ over the time course of the titration (≈20 min duration) as ascertained by analytical HPLC. The absorbance at 621 nm versus the [Zn(II)] / [S100A7] ratio was plotted. Each experiment was performed in triplicate and data from representative trials are presented.

Zinc Competition Assays with S100A7 and FZ3. A 1-mL solution containing FZ3 (2 μM) and S100A7 (2 μM) was prepared in a PMMA cuvette (75 mM HEPES, 100 mM NaCl, pH 7.0). The solution was mixed gently and incubated for 1 h in the dark at room temperature. The emission spectrum of the solution was then recorded. An aliquot of Zn(II) was subsequently added to the sample to a final concentration of 2 μM, the solution was gently mixed, and

incubated for 2.5 h in the dark at room temperature. The emission spectrum of the solution was then recorded. The sample was excited at 494 nm, and the emission was monitored from 505–650 nm and integrated over this range. Each experiment was performed in triplicate. The mean and SDM values are reported.

Zinc Competition Titrations with S100A7 and ZP4. Competition experiments with S100A7 and ZP4 were employed to determine the apparent dissociation constant values of S100A7 for Zn(II) at pH 7.0. ZP4 (ε_{506} = 61 000 $M^{-1}cm^{-1}$)[6] was diluted to 2 μM in a total volume of 2 mL (75 mM HEPES, 100 mM NaCl, pH 7.0, ± 2 mM Ca(II)). After the optical absorption and emission spectra of the ZP4 solution were recorded, S100A7 was added to a final concentration of 5 μM, and the optical absorption and emission spectra were recorded again to check that they were unperturbed by addition of the protein sample. The ZP4/S100A7 mixture was titrated with Zn(II) in 0.5 μM increments (1 μL from a 1-mM Zn(II) stock solution), the emission spectrum was recorded from 505 to 650 nm (λ_{ex} = 495 nm), and integrated over this range. The samples were allowed to equilibrate for ≈2 min between each Zn(II) addition. Normalized integrated emission versus the concentration of Zn(II) added was plotted, and the resulting titration curve was fit to one- and two-binding site models using the DynaFit software and a custom script previously described.[7] Each titration was performed in triplicate. The mean and SDM values are reported.

Co(II)-binding Titrations and Metal Substitution Assays. Protein samples (300 μM, 400 μL) were prepared in 75 mM HEPES, 100 mM NaCl, pH 7.0 and the absorption spectrum recorded. Co(II) was then added in 75-μM increments (1 μL from a 30-mM stock) and the solution was gently mixed. The optical absorption spectrum was recorded, and the extinction coefficient calculated from the protein concentration. Co(II)-binding titrations with $S100A7_{red}$ were carried out aerobically, and protein was analyzed by HPLC before and after the titration to confirm that air oxidation of the disulfide bond did not occur during the experiment. For metal

substitution experiments, a solution containing S100A7 (300 μM) and Co(II) (1.2 mM, 4.0 equiv) was prepared (75 mM HEPES, 100 mM NaCl, pH 7.0) and the optical absorption spectrum recorded. Then, Zn(II) was added (1.2 mM, 4.0 equiv) from a 100-mM stock solution, and the optical absorption spectra were recorded over a 20-h time period. For metal substitution experiments with $S100A7_{red}$, the Co(II)-bound protein sample was prepared anaerobically in a septum-capped quartz cuvette in the glovebox. The sample was removed from the glovebox and the absorption spectrum was recorded. An aliquot of Zn(II) (1.2 mM, 4.0 equiv) was then added by syringe transfer, and the optical absorption spectra recorded. The protein was analyzed by HPLC before and after the displacement experiment to confirm that air oxidation of the disulfide bond did not occur. Each Co(II)-binding titration and metal displacement experiment was performed at least in duplicate and data from representative trials are shown.

Metal Analysis (ICP-MS). For the metal-depletion experiments, 1 mL of TSB:Tris (32:68 (v:v) ratio) was transferred to 5-mL centrifuge tubes (Argos). Protein samples were buffer-exchanged into AMA buffer (20 mM Tris-HCl, 100 mM NaCl, pH 7.5) using 0.5-mL 10 MWCO Amicon spin concentrators, and diluted to final concentrations of 31.25, 62.5, 125, 250, and 500 μg/mL in the TSB:Tris medium. Untreated TSB:Tris containing no protein and the S100A7-treated samples were incubated for 20 h (30 ^{o}C, 150 rpm). The samples were spin filtered using the 4-mL Amicon spin concentrators (3750 rpm, 30 min). The flow through was collected (900 μL) and diluted 1:1 with 3% HNO_3 nitric acid. Samples were analyzed at the Center for Environmental Health Sciences (CEHS) Core Facility at MIT. The concentrations of Mg, Ca, Fe, Mn, Co, Ni, Cu, and Zn were quantified employing an Agilent 7900 ICP-MS used in Helium mode outfitted with integrated autosampler (I-AS). An internal standard of terbium (Agilent) was used to control for sample effects, and the concentrations of analyte were calibrated using standards prepared by serial dilution of the Agilent Environmental Calibration Standard mix. All experiments were performed three times with at least two different starting stocks of media and protein. The mean and SDM values are reported.

Antibacterial Activity Assays (AMA). For these studies, TSB:Tris, MRS:Tris, and BHI:Tris AMA media were composed of 32:68 (v:v) ratio of TSB/MRS/BHI and AMA buffer (20 mM Tris-HCl, 100 mM NaCl, pH 7.5). The growth inhibitory activity of S100A7 against bacterial strains was investigated by following literature protocols.[7, 8] Bacterial strain stocks were stored at -80 ^{o}C in media containing 25% glycerol. AMA medium (TSB:Tris for *Escherichia coli*, *Staphylococcus aureus, Pseudomonas aeruginosa;* MRS:Tris for *Lactobacillus plantarum*; and BHI:Tris for *Listeria monocytogenes*) was prepared using sterile technique. The growth medium (TSB:Tris for *E. coli*, *S. aureus, P. aeruginosa;* MRS:Tris for *L. plantarum*; and BHI:Tris for *L. monocytogenes*) was inoculated with a single colony and grown overnight (37 ^{o}C, t ≈ 16 h) on a rotating wheel. The overnight cultures were then diluted 1:100 in a culture tube containing 5 mL of medium and allowed to grow to mid-log phase at an OD_{600} ≈ 0.6 (t ≈ 2 - 3 h). The cultures at mid-log phase were diluted 1:500 into AMA medium, and 90 μL of the dilution was added to a well containing 10 μL of 10x protein in AMA buffer in 96-well round-bottom plates (Corning, Inc.). For samples containing a ≈2-mM Ca(II) supplement, the Tris buffer was supplemented with 3 mM Ca(II). Each condition was repeated in three wells. The plate was covered with a wet paper towel and wrapped with Saran wrap. The plate was then allowed to incubate in an incubator-shaker (37 ^{o}C for *E. coli, S. aureus,* and *P. aeruginosa;* 30 ^{o}C for *L. plantarum* and *L. monocytogenes*, 150 rpm, t=20 h). Bacterial growth was monitored by OD_{600} at regular intervals using a plate reader. Each set of experiments was performed at least three times with at least two different protein and media stocks. The mean and SDM are reported.

The microdilution AMA presented in Figure S22 was performed according to a literature protocol.[9]

Table S1. Extinction coefficients for S100A7 monomers

Protein	Description	ε_{280} (M^{-1} cm^{-1})[a]
$S100A7_{ox}$	Oxidized; Cys47–Cys96 disulfide bond	4595
$S100A7\Delta_{ox}$	(H18A)(D25A)(H87A)(H91A) variant Oxidized; Cys47–Cys96 disulfide bond	4595
$S100A7_{red}$	Reduced; Cys47 and Cys96 free thiols	4470
$S100A7\Delta_{red}$	(H18A)(D25A)(H87A)(H91A) variant Reduced; Cys47 and Cys96 free thiols	4470
S100A7-Ser	(C47S)(S96S) variant	4470
S100A7-Ala	(C47A)(S96A) variant	4470

[a] Extinction coefficients (280 nm) were calculated by using the ProtParam tool available on the ExPASy server (http://web.expasy.org/protparam).

Table S2. Metal analysis (ICP-MS) of S100A7 from representative protein purifications

Metal	Protein (10 μM)				
	$S100A7_{ox}$	**$S100A7_{red}$**	**S100A7-Ser**	**S100A7-Ala**	**$S100A7\Delta_{ox}$**
Mg (μM)	1.525	1.844	0.825	1.236	0.702
(equiv)	0.153	0.184	0.083	0.124	0.070
Ca (μM)	0.543	1.039	13.3	6.733	12.95
(equiv)	0.054	0.104	1.33	0.673	1.300
Mn (μM)	0.040	0.052	0.009	0.022	0.0174
(equiv)	0.004	0.005	0.000	0.002	0.002
Fe (μM)	0.379	0.486	0.086	0.965	0.0836
(equiv)	0.038	0.049	0.009	0.097	0.008
Co (μM)	0.001	0.002	0.003	0.001	0.002
(equiv)	0.000	0.000	0.000	0.000	0.000
Ni (μM)	0.314	0.324	0.077	0.205	0.065
(equiv)	0.031	0.03	0.008	0.021	0.007
Cu (μM)	0.057	0.033	0.045	0.427	0.018
(equiv)	0.006	0.003	0.005	0.043	0.002
Zn (μM)	0.416	0.383	0.602	0.604	0.030
(equiv)	0.042	0.038	0.06	0.060	0.003

Table S3. Analytical SEC elution volumes and calculated molecular weights[a]

Protein	Ca(II)	Elution Volume (mL)	Calculated Molecular Weight (kDa)
$S100A7_{ox}$	-	12.7	24.2
$S100A7_{ox}$	+	12.7	26.4
$S100A7_{red}$	-	12.3	27.6
$S100A7_{red}$	+	12.4	25.8
S100A7-Ser	-	12.0	22.1
S100A7-Ser	+	12.2	23.1
S100A7-Ala	-	11.9	21.4
S100A7-Ala	+	12.0	22.1

[a] Each sample contained 30 μM protein (75 mM HEPES, 100 mM NaCl, pH 7.0). The +Ca(II) samples contained 2 mM Ca(II) in the sample and running buffer. The experiments were performed at 4 °C.

Table S4. Fits for apparent $K_{d,Zn}$ values from ZP4 competition **t**itrations with S100A7 variants

Protein	Ca(II) [a]	Apparent $K_{d,Zn}$ (pM)		
		One site	Two sites $K_{d1} = K_{d2}$	Two sites $K_{d1} \neq K_{d2}$
$S100A7_{ox}$	-	400 ± 14	430 ± 13	290 ± 20
				580 ± 31
	+	605 ± 20	580 ± 40	320 ± 28
				1100 ± 89
$S100A7_{red}$	-	730 ± 41	660 ± 56	280 ± 18
				3500 ± 310
	+	400 ± 20	420 ± 41	300 ± 26
				570 ± 39
S100A7-Ser	-	740 ± 49	700 ± 58	470 ± 77
				2070 ± 950
	+	350 ± 25	370 ± 11	350 ± 42
				400 ± 37
S100A7-Ala	-	500 ± 29	500 ± 69	260 ± 42
				990 ± 120
	+	490 ± 28	490 ± 21	330 ± 36
				710 ± 70

[a] For the +Ca(II) samples, 100 equiv of Ca(II) (500 μM) were added to the buffer. For the –Ca(II) samples, no Ca(II) was added to the buffer. Metal analysis (ICP-MS) showed the buffer employed in the –Ca(II) experiments contained less than 100 nM Ca.

Table S5. Metal Analysis of untreated Tris:TSB medium in the presence and absence of a 2-mM Ca(II) supplement (mean ± SDM, *n* = 3)

Element	–Ca(II) (ppm)	–Ca(II) (μM)	+Ca(II) (ppm)	+Ca(II) (μM)
Mg	4300 ± 400	180 ± 17	4000 ± 165	170 ± 19
Ca	4100 ± 95	102 ± 2.4	9500 ± 2600	2400 ± 65
Mn	12 ± 3.0	0.02 ± 0.06	10 ± 3.3	0.20 ± 0.06
Fe	2.9 ± 0.21	160 ± 12	2.8 ± 0.3	160 ± 14
Co	2.8 ± 0.31	0.050 ± 0.006	2.5 ± 0.23	0.040 ± 0.004
Ni	39 ± 6.9	0.67 ± 0.12	434 ± 10.3	0.750 ± 0.18
Cu	0.16 ± 0.039	10 ± 2.5	0.16 ± 0.05	10 ± 2.9
Zn	260 ± 37	4.0 ± 0.56	260 ± 20	3.9 ± 0.30

Table S6. Metal Analysis of Tris:TSB medium treated with 31.25 μg/mL of $S100A7_{ox}$ in the presence and absence of a 2-mM Ca(II) supplement (mean ± SDM, *n* = 3)

Element	–Ca(II) (ppm)	–Ca(II) (μM)	+Ca(II) (ppm)	+Ca(II) (μM)
Mg	4400 ± 400	180 ± 18	4200 ± 330	170 ± 13
Ca	4300 ± 230	110 ± 6.1	10000 ± 8500	2500 ± 210
Mn	12 ± 2.8	0.2 ± 0.05	12 ± 5.7	0.2 ± 0.10
Fe	3.0 ± 0.16	160 ± 11	2.8 ± 0.29	160 ± 16
Co	2.8 ± 0.29	0.050 ± 0.005	2.7 ± 0.41	0.050 ± 0.007
Ni	40 ± 12	0.7 + 0.21	44 ± 12.2	0.70 ± 0.21
Cu	0.150 ± 0.043	9 ± 2.7	0.15 ± 0.052	10 ± 3.3
Zn	230 ± 39	3.5 ± 0.60	190 ± 54	2.9 ± 0.83

Table S7. Metal Analysis of Tris:TSB medium treated with 62.5 μg/mL of $S100A7_{ox}$ in the presence and absence of a 2-mM Ca(II) supplement (mean ± SDM, *n* = 3)

Element	–Ca(II) (ppm)	–Ca(II) (μM)	+Ca(II) (ppm)	+Ca(II) (μM)
Mg	4300 ± 160	178 ± 7	4100 ± 59	170 ± 3
Ca	4200 ± 200	106 ± 5	10100 ± 4500	2430 ± 17
Mn	15 ± 4.5	0.26 ± 0.08	11 ± 3.0	0.20 ± 0.05
Fe	170 ± 9	3.0 ± 0.16	170 ± 11	3.0 ± 0.20
Co	2.8 ± 0.17	0.047 ± 0.003	2.6 ± 0.23	0.04 ± 0.004
Ni	39 ± 7.7	0.7 ± 0.13	46 ± 8.4	0.8 ± 0.14
Cu	0.15 ± 0.05	10 ± 3.1	0.15 ± 0.056	10 ± 3.6
Zn	82 ± 15	1.3 ± 0.22	110 ± 29	1.8 ± 0.44

Table S8. Metal Analysis of Tris:TSB medium treated with 125 μg/mL of $S100A7_{ox}$ in the presence and absence of a 2-mM Ca(II) supplement (mean ± SDM, *n* = 3)

Element	–Ca(II) (ppm)	–Ca(II) (μM)	+Ca(II) (ppm)	+Ca(II) (μM)
Mg	4200 ± 170	175 ± 7	4200 ± 250	175 ± 10
Ca	4300 ± 300	107 ± 8	97000 ± 680	2500 ± 110
Mn	13 ± 3.4	0.23 ± 0.06	14 ± 4.7	0. ± 0.10
Fe	172 ± 6	3.1 ± 0.10	176 ± 4	3.15 ± 0.07
Co	2.8 ± 0.17	0.049 ± 0.004	2.6 ± 0.23	0.049 ± 0.003
Ni	40 ± 7.7	0.7 ± 0.13	37 ± 3.7	0.63 ± 0.063
Cu	0.15 ± 0.034	10 ± 3.4	0.015 ± 0.048	10 ± 3.1
Zn	44 ± 9.4	0.7 ± 0.14	60 ± 20	0.9 ± 0.31

Table S9. Metal Analysis of Tris:TSB medium treated with 250 μg/mL of $S100A7_{ox}$ in the presence and absence of a 2-mM Ca(II) supplement (mean ± SDM, *n* = 3)

Element	–Ca(II) (ppm)	–Ca(II) (μM)	+Ca(II) (ppm)	+Ca(II) (μM)
Mg	4000 ± 170	170 ± 19	4200 ± 250	170 ± 2.5
Ca	4200 ± 200	110 ± 13	101000 ± 4500	2430 ± 17
Mn	12 ± 3.1	0.21 ± 0.06	12 ± 3.4	0.21 ± 0.06
Fe	170 ± 21	3.0 ± 0.38	170 ± 15	3.1 ± 0.26
Co	2.9 ± 0.22	0.049 ± 0.006	2.8 ± 0.17	0.049 ± 0.003
Ni	44 ± 6.9	0.7 ± 0.12	37 ± 1.1	0.63 ± 0.019
Cu	0.14 ± 0.034	9 ± 2.2	0.015 ± 0.046	10 ± 2.9
Zn	39 ± 16	0.6 ± 0.25	43 ± 18	0.6 ± 0.28

Table S10. Metal Analysis of Tris:TSB medium treated with 500 μg/mL of $S100A7_{ox}$ in the presence and absence of a 2-mM Ca(II) supplement (mean ± SDM, *n* = 3)

Element	–Ca(II) (ppm)	–Ca(II) (μM)	+Ca(II) (ppm)	+Ca(II) (μM)
Mg	4200 ± 460	166 ± 7	4000 ± 80	165 ± 4
Ca	4300 ± 530	2370 ± 65	9500 ± 6700	2400 ± 170
Mn	11 ± 3.2	0.21 ± 0.06	10 ± 3.6	0.19 ± 0.06
Fe	160 ± 11	2.9 ± 0.20	162 ± 2	2.91 ± 0.03
Co	2.5 ± 0.23	0.049 ± 0.004	2.8 ± 0.29	0.049 ± 0.008
Ni	37 ± 1.4	0.63 ± 0.024	38 ± 4.2	0.64 ± 0.072
Cu	0.14 ± 0.036	9 ± 2.3	0.12 ± 0.026	8 ± 1.7
Zn	36 ± 2.8	0.56 ± 0.04	38 ± 3.2	0.58 ± 0.05

Table S11. Metal Analysis of Tris:TSB medium treated with 31.25 μg/mL of S100A7-Ser in the presence and absence of a 2-mM Ca(II) supplement (mean ± SDM, *n* = 3)

Element	–Ca(II) (ppm)	–Ca(II) (μM)	+Ca(II) (ppm)	+Ca(II) (μM)
Mg	4400 ± 550	180 ± 23	4100 ± 360	170 ± 15
Ca	4100 ± 360	102 ± 9.1	95000 ± 7400	2400 ± 190
Mn	11 ± 3.2	0.21 ± 0.058	10 ± 3.6	0.19 ± 0.065
Fe	160 ± 11	2.9 ± 0.20	162 ± 2	2.91 ± 0.03
Co	3.0 ± 0.21	0.051 ± 0.004	2.6 ± 0.38	0.044 ± 0.006
Ni	43 ± 6.5	0.73 ± 0.11	44 ± 4.9	0.75 ± 0.084
Cu	9 ± 2.3	0.14 ± 0.04	10 ± 2.0	0.15 ± 0.032
Zn	140 ± 47	2.2 ± 0.72	140 ± 50	2.1 ± 0.77

Table S12. Metal Analysis of Tris:TSB medium treated with 62.5 μg/mL of S100A7-Ser in the presence and absence of a 2-mM Ca(II) supplement (mean ± SDM, *n* = 3)

Element	–Ca(II) (ppm)	–Ca(II) (μM)	+Ca(II) (ppm)	+Ca(II) (μM)
Mg	4400 ± 320	180 ± 13	4400 ± 250	180 ± 11
Ca	4000 ± 420	100 ± 10	104000 ± 5600	2600 ± 140
Mn	13 ± 3.8	0.22 ± 0.068	12 ± 2.6	0.22 ± 0.047
Fe	170 ± 19	3.1 ± 0.34	171 ± 6	3.1 ± 0.11
Co	2.94 ± 0.04	0.050 ± 0.001	2.9 ± 0.29	0.049 ± 0.005
Ni	45 ± 3.2	0.77 ± 0.054	49.3 ± 0.5	0.840 ± 0.007
Cu	13 ± 3.0	0.21 ± 0.047	12 ± 1.2	0.18 ± 0.019
Zn	40 ± 18	0.7 ± 0.27	80 ± 44	0.7 ± 0.18

Table S13. Metal Analysis of Tris:TSB medium treated with 125 μg/mL of S100A7-Ser in the presence and absence of a 2-mM Ca(II) supplement (mean ± SDM, *n* = 3)

Element	–Ca(II) (ppm)	–Ca(II) (μM)	+Ca(II) (ppm)	+Ca(II) (μM)
Mg	4300 ± 420	180 ± 18	4300 ± 270	180 ± 11
Ca	4000 ± 280	100 ± 10	102000 ± 4300	2500 ± 110
Mn	12 ± 3.0	0.21 ± 0.06	11 ± 2.6	0.21 ± 0.048
Fe	177 ± 7	3.2 ± 0.13	170 ± 16	3.1 ± 0.29
Co	29.0 ± 0.27	0.05 ± 0.001	2.7 ± 0.18	0.045 ± 0.003
Ni	46 ± 5	0.78 ± 0.086	47 ± 3.3	0.80 ± 0.056
Cu	10 ± 3.4	0.15 ± 0.053	12 ± 1.2	0.18 ± 0.018
Zn	44 ± 9.9	0.7 ± 0.15	40 ± 12	0.67 ± 0.18

Table S14. Metal Analysis of Tris:TSB medium treated with 250 μg/mL of S100A7-Ser in the presence and absence of a 2-mM Ca(II) supplement (mean ± SDM, *n* = 3)

Element	–Ca(II) (ppm)	–Ca(II) (μM)	+Ca(II) (ppm)	+Ca(II) (μM)
Mg	4300 ± 480	180 ± 18	4400 ± 270	180 ± 11
Ca	4200 ± 320	100 ± 7	104000 ± 4900	2600 ± 120
Mn	11 ± 2.9	0.20 ± 0.052	11 ± 2.9	0.20 ± 0.053
Fe	172 ± 2	3.07 ± 0.036	170 ± 22	3.0 ± 0.39
Co	3.0 ± 0.33	0.049 ± 0.005	2.9 ± 0.23	0.049 ± 0.004
Ni	47 ± 3.3	0.80 ± 0.06	46 ± 3.9	0.78 ± 0.066
Cu	12.4 ± 0.4	0.194 ± 0.005	12 ± 0.6	0.186 ± 0.009
Zn	40 ± 15	0.7 ± 0.23	40 ± 11	0.63 ± 0.16

Table S15. Metal Analysis of Tris:TSB medium treated with 500 μg/mL of S100A7-Ser in the presence and absence of a 2-mM Ca(II) supplement (mean ± SDM, *n* = 3)

Element	–Ca(II) (ppm)	–Ca(II) (μM)	+Ca(II) (ppm)	+Ca(II) (μM)
Mg	4500 ± 550	180 ± 20	4300 ± 267	180 ± 11
Ca	4600 ± 720	105 ± 8	102000 ± 5100	2600 ± 130
Mn	11 ± 1.6	0.21 ± 0.028	11 ± 3.1	0.19 ± 0.056
Fe	180 ± 15	3.2 ± 0.26	174 ± 9	3.1 ± 0.16
Co	3.1 ± 0.38	0.050 ± 0.006	2.9 ± 0.20	0.049 ± 0.004
Ni	46 ± 4.1	0.78 ± 0.07	52.0 ± 0.34	0.886 ± 0.006
Cu	11 ± 1.1	0.18 ± 0.017	12 ± 1.3	0.19 ± 0.020
Zn	37 ± 2.9	0.56 ± 0.044	37 ± 5.5	0.57 ± 0.083

Table S16. Metal Analysis of Tris:TSB medium treated with 31.25 μg/mL of S100A7-Ala in the presence and absence of a 2-mM Ca(II) supplement (mean ± SDM, *n* = 3)

Element	–Ca(II) (ppm)	–Ca(II) (μM)	+Ca(II) (ppm)	+Ca(II) (μM)
Mg	3700 ± 350	150 ± 14	4200 ± 600	180 ± 25
Ca	3600 ± 300	90 ± 7.5	94750 ± 480	2400 ± 325
Mn	12 ± 0.9	0.21 ± 0.017	10.8 ± 0.7	0.196 ± 0.011
Fe	150 ± 12	2.7 ± 0.21	159 ± 10	2.8 ± 0.17
Co	2.9 ± 0.23	0.049 ± 0.004	3.0 ± 0.28	0.051 ± 0.005
Ni	45 ± 9.3	0.7 ± 0.16	46 ± 6.0	0.8 ± 0.11
Cu	11 ± 3.2	0.18 ± 0.05	13 ± 1.7	0.20 ± 0.026
Zn	110 ± 26	1.7 ± 0.41	100 ± 17	1.7 ± 0.26

Table S17. Metal Analysis of Tris:TSB medium treated with 62.5 μg/mL of S100A7-Ala in the presence and absence of a 2-mM Ca(II) supplement (mean ± SDM, *n* = 3)

Element	–Ca(II) (ppm)	–Ca(II) (μM)	+Ca(II) (ppm)	+Ca(II) (μM)
Mg	3900 ± 440	170 ± 19	4100 ± 140	170 ± 5.8
Ca	4000 ± 340	99 ± 8.4	96300 ± 830	400 ± 430
Mn	11.8 ± 0.9	0.22 ± 0.029	12 ± 1.4	0.21 ± 0.025
Fe	160 ± 14	2.8 ± 0.25	160 ± 9.5	2.8 ± 0.17
Co	3.0 ± 0.30	0.051 ± 0.005	2.9 ± 0.13	0.051 ± 0.005
Ni	40 ± 10	0.65 ± 0.17	44 ± 4.0	0.76 ± 0.068
Cu	10 ± 2.3	0.16 ± 0.037	11 ± 1.7	0.2 ± 0.27
Zn	38 ± 4.2	0.60 ± 0.066	42 ± 9.2	0.7 ± 0.15

Table S18. Metal Analysis of Tris:TSB medium treated with 125 μg/mL of S100A7-Ala in the presence and absence of a 2-mM Ca(II) supplement (mean ± SDM, *n* = 3)

Element	–Ca(II) (ppm)	–Ca(II) (μM)	+Ca(II) (ppm)	+Ca(II) (μM)
Mg	4200 ± 640	170 ± 27	4100 ± 300	170 ± 12
Ca	37100± 680	90 ± 17	97000 ± 7300	2400 ± 180
Mn	13 ± 1.6	0.23 ± 0.029	12 ± 2.0	0.21 ± 0.036
Fe	160 ± 12	2.8 ± 0.21	160 ± 6.9	2.9 ± 0.122
Co	3.1 ± 0.36	0.053 ± 0.006	3.0 ± 0.25	0.051 ± 0.004
Ni	42 ± 1.2	0.72 ± 0.02	45 ± 6.4	0.8 ± 0.11
Cu	11 ± 3.2	0.18 ± 0.050	11.2 ± 0.8	0.18 ± 0.012
Zn	34 ± 2.1	0.53 ± 0.033	37 ± 4.4	0.6 ± 0.70

Table S19. Metal Analysis of Tris:TSB medium treated with 250 μg/mL of S100A7-Ala in the presence and absence of a 2-mM Ca(II) supplement (mean ± SDM, *n* = 3)

Element	–Ca(II) (ppm)	–Ca(II) (μM)	+Ca(II) (ppm)	+Ca(II) (μM)
Mg	4000 ± 440	170 ± 19	4200 ± 109	174 ± 4.5
Ca	3700 ± 470	90 ± 12	100000 ±3400	2500 ± 180
Mn	13 ± 1.8	0.24 ± 0.046	12 ± 2.7	0.22 ± 0.047
Fe	180 ± 31	3.2 ± 0.55	180 ± 26	3.2 ± 0.47
Co	3.1 ± 0.39	0.053 ± 0.006	3.1 ± 0.17	0.051 ± 0.004
Ni	40 ± 5.2	0.69 ± 0.089	47 ± 3.1	0.80 ± 0.053
Cu	10 ± 2.2	0.16 ± 0.035	10.0 ± 0.4	0.161 ± 0.002
Zn	40 ± 17	0.7 ± 0.27	30.9 ± 0.90	0.49 ± 0.014

Table S20. Metal Analysis of Tris:TSB medium treated with 500 μg/mL of S100A7-Ala in the presence and absence of a 2-mM Ca(II) supplement (mean ± SDM, *n* = 3)

Element	–Ca(II) (ppm)	–Ca(II) (μM)	+Ca(II) (ppm)	+Ca(II) (μM)
Mg	3900 ± 320	160 ± 13	4300 ± 320	180 ± 13.
Ca	61000 ± 490	1830 ± 12	100000 ± 3400	1000 ± 200
Mn	13 ± 2.5	0.23 ± 0.033	12 ± 2.6	0.22 ± 0.050
Fe	180 ± 29	3.2 ± 0.51	180 ± 28	3.2 ± 0.49
Co	3.1 ± 0.39	0.052 ± 0.006	3.1 ± 0.17	0.054 ± 0.006
Ni	44 ± 8.7	0.7 ± 0.15	50 ± 1.6	0.8 ± 0.28
Cu	10 ± 2.2	0.16 ± 0.035	10.2 ± 0.11	0.161 ± 0.002
Zn	37 ± 9.8	0.6 ± 0.15	31.2 ± 0.5	0.491 ± 0.008

Table S21. Strains and growth conditions employed in this work

Strain	Source	Culture conditions[a]
E. coli K-12	Keio Collection[10]	TSB/Tris (32:68 v/v), 37 °C, 150 rpm
E. coli K-12 Δ*znuA*	Keio Collection[10]	TSB/Tris (32:68 v/v), 37 °C, 150 rpm
E. coli 25922	ATCC	TSB/Tris (32:68 v/v), 37 °C, 150 rpm
L. plantarum WCSF1	ATCC	MRS/Tris (32:68 v/v). 30 °C, 150 rpm
L. monocytogenes ATCC 19115	ATCC	BHI/Tris (32:68 v/v), 30 °C, 150 rpm
P. aeruginosa PAO1	Manoil Laboratory[b]	TSB/Tris (32:68 v/v), 37 °C, 150 rpm
S. aureus ATCC 25923	ATCC	TSB/Tris (32:68 v/v), 37 °C, 150 rpm

[a] All media contained dextrose. These are the culture conditions employed for the antimicrobial activity assays. [b] University of Washington (Seattle, WA).

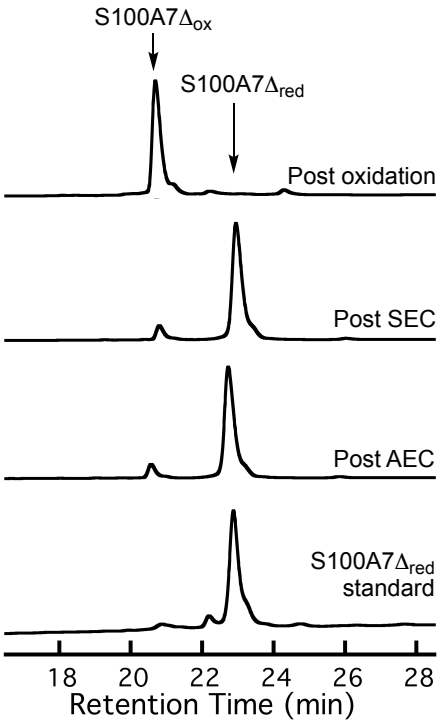

Figure S1. Analytical HPLC traces (220 nm absorption) showing the speciation of S100A7Δ at different steps of the protein purification and following Cu(II)-catalyzed oxidation. The protein purification involves purification of S100A7Δ by AEC and SEC. Conditions: 9 μM protein, 100 μL injection volume. Each trace was normalized to a maximum peak absorbance of 1. The shoulder peaks observed in the chromatograms of $S100A7\Delta_{ox}$ and $S100A7\Delta_{red}$ correspond to the isoforms of S100A7Δ missing the N-terminal methionine.

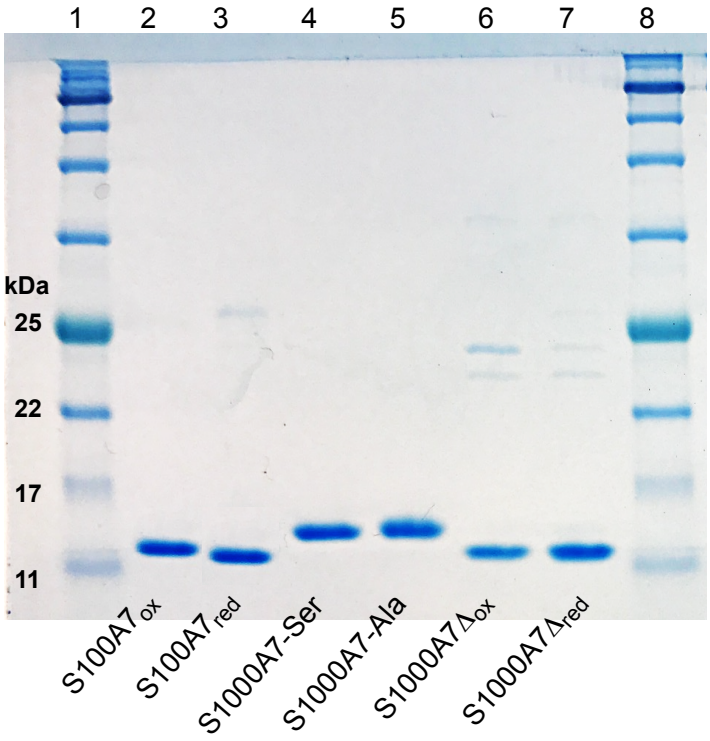

Figure S2. SDS-PAGE purity gel (13% Tris-HCl, tricine gel) of the S100A7 variants employed in this work. Ladder: P7712s color prestained protein standard broad range (New England Biolabs). Ladder (lane 1), $S100A7_{ox}$ (lane 2), $S100A7_{red}$ (lane 3), S100A7-Ser (lane 4), S100A7-Ala (lane 5), $S100A7\Delta_{ox}$ (lane 6), $S100A7\Delta_{red}$ (lane 7), and ladder (lane 8).

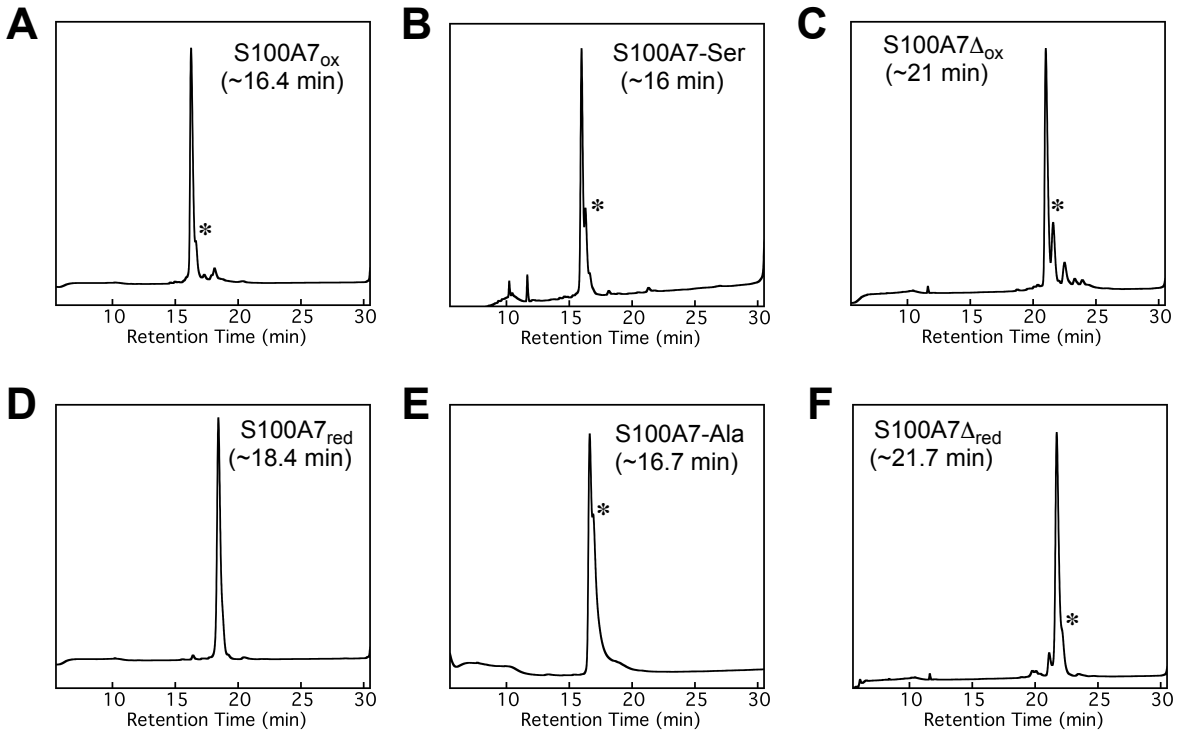

Figure S3. HPLC chromatograms (220 nm absorption) of S100A7 variants: (A) $S100A7_{ox}$, (B) S100A7-Ser, (C) $S100A7\Delta_{ox}$, (D) $S100A7_{red}$, (E) S100A7-Ala, and (F) $S100A7\Delta_{red}$. Conditions: 9 μM protein, 100 μL injection volume. An asterisk (*) indicates the position of the isoform of S100A7 missing the N-terminal methionine.

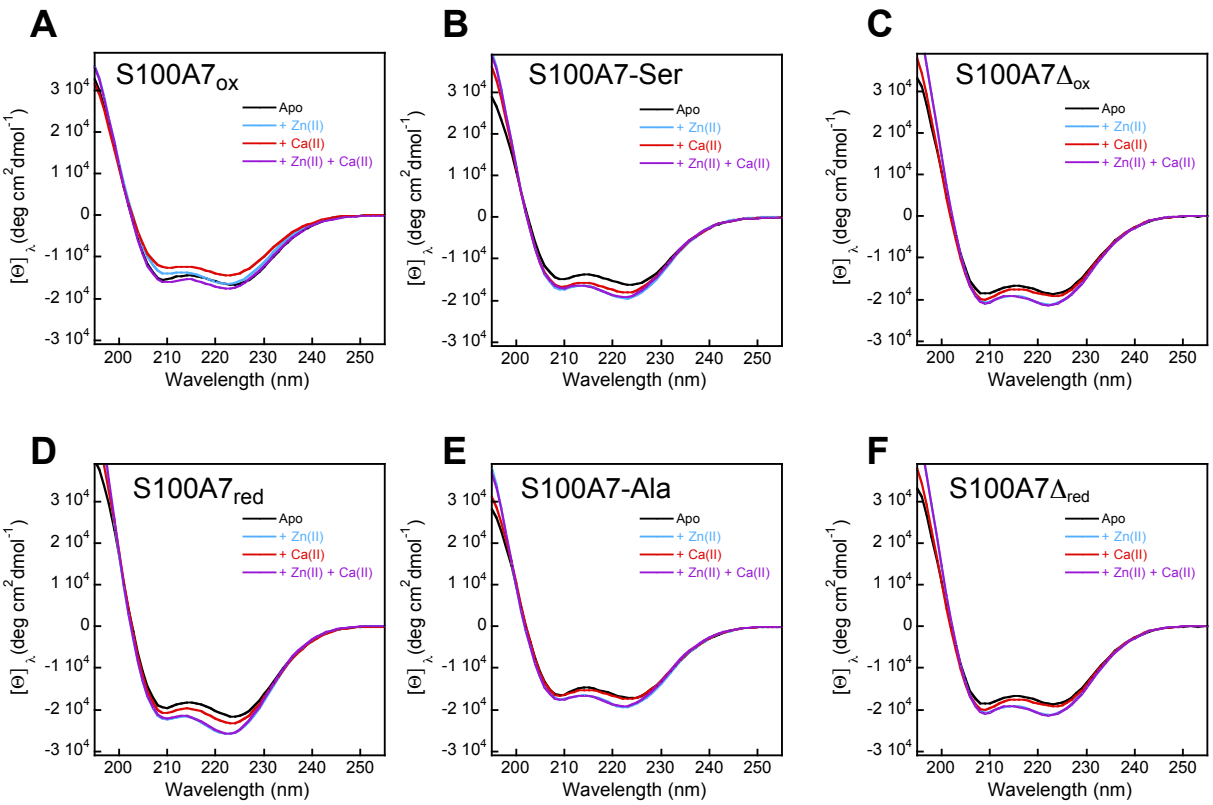

Figure S4. CD spectra of 10 μM of (A) $S100A7_{ox}$, (B) S100A7-Ser, (C) $S100A7\Delta_{ox}$, (D) $S100A7_{red}$, (E) S100A7-Ala, and (F) $S100A7\Delta_{red}$ in the absence and presence of divalent cations (1 mM Tris-HCl, pH 7.5, T = 25°C). Black trace, without metal addition; blue trace, in the presence of 20 μM Zn(II); red trace, in the presence of 2 mM Ca(II); purple trace, in the presence of 20 μM Zn(II) and 2 mM Ca(II).

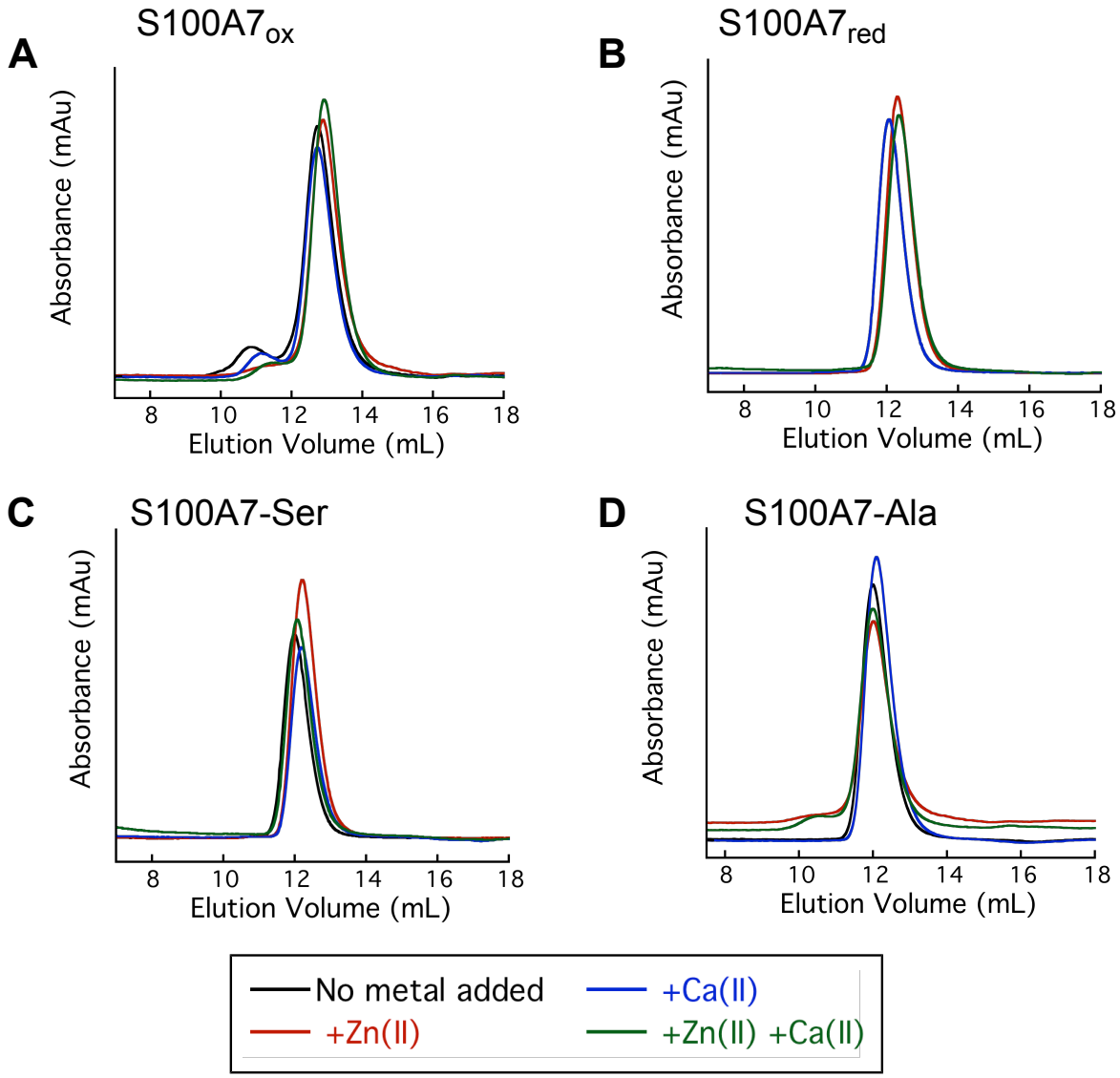

Figure S5. Analytical size exclusion chromatography (SEC) of S100A7 (30 μM, 300 μL) in the absence and presence of divalent cations (75 mM HEPES, 100 mM NaCl, pH 7.0). (A) $S100A7_{ox}$, (B) $S100A7_{red}$, (C) S100A7-Ser, and (D) S100A7-Ala. For experiments containing Zn(II) and Ca(II), 2 equiv of Zn(II) were added to the samples, and 2 mM Ca(II) were added to the sample and running buffer. The absorbance was monitored at 280 nm.

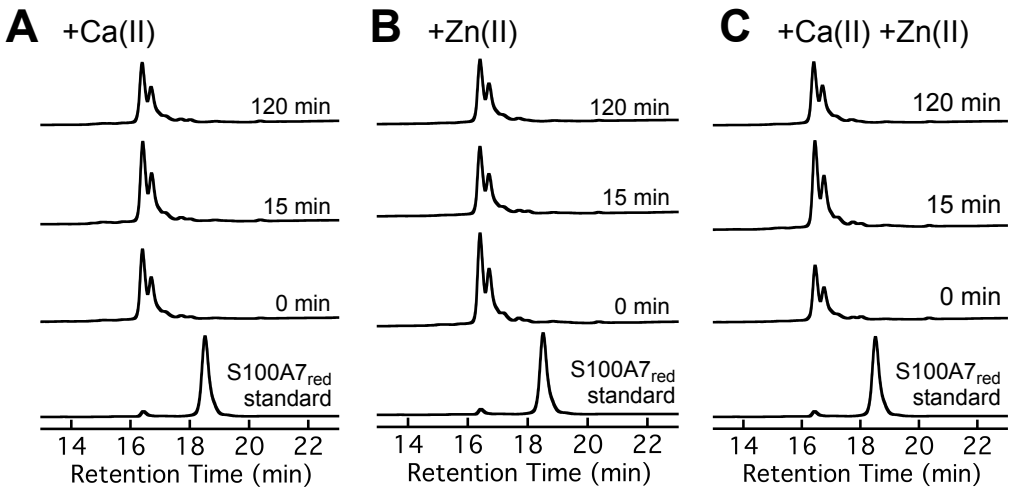

Figure S6. Analytical HPLC traces (220 nm) for the no enzyme controls for the Trx/TrxR activity assays presented in Figure 3C-E of the main text. (A) $S100A7_{ox}$ and 2 mM Ca(II), (B) $S100A7_{ox}$ and 1.9 equiv of Zn(II), and (C) $S100A7_{ox}$ and 1.9 equiv of Zn(II) and 2 mM Ca(II). Both Trx and TrxR were omitted from the assay mixture. Conditions: 5 μM $S100A7_{ox}$, 1 mM NADPH, ±Ca(II), ±Zn(II); 75 mM HEPES, 100 mM NaCl, pH 7.0. Two peaks are observed for $S100A7_{ox}$ because two isoforms of S100A7 are present (±N-Met).

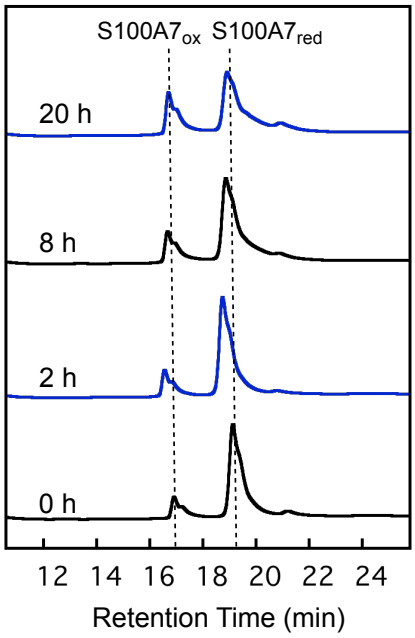

Figure S7. Analytical HPLC (220 nm) showing air oxidation of $S100A7_{red}$ over time (0, 2, 8, and 20 h). A 500-μL aliquot of 30 μM $S100A7_{red}$ in 75 mM HEPES, 100 mM NaCl, pH 7.0 was incubated at room temperature, and 100-μL aliquots were analyzed by HPLC at the specified timepoints. The shoulder peak observed corresponds to the isoform of S100A7 missing the N-terminal methionine.

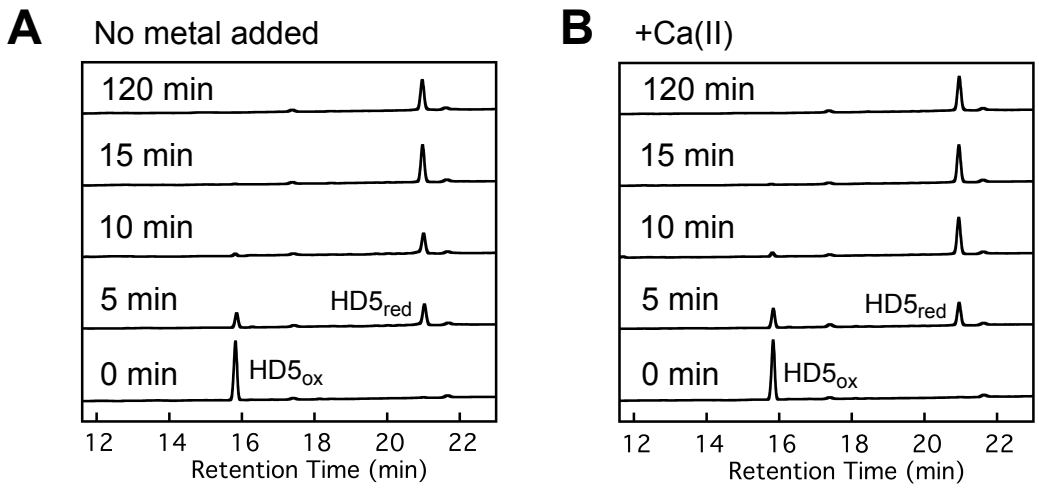

Figure S8. Analytical HPLC traces (220 nm) monitoring the reduction of $HD5_{ox}$ by Trx/TrxR in the (A) absence and (B) presence of 2 mM Ca(II). These assays served as controls for examining the effect of 2 mM Ca(II) on the activity of the thioredoxin system. Conditions: 10 μM $HD5_{ox}$, 1 μM human Trx, 0.1 μM rat liver TrxR, 1 mM NADPH, ±2 mM Ca(II), 75 mM HEPES, 100 mM NaCl, pH 7.0.

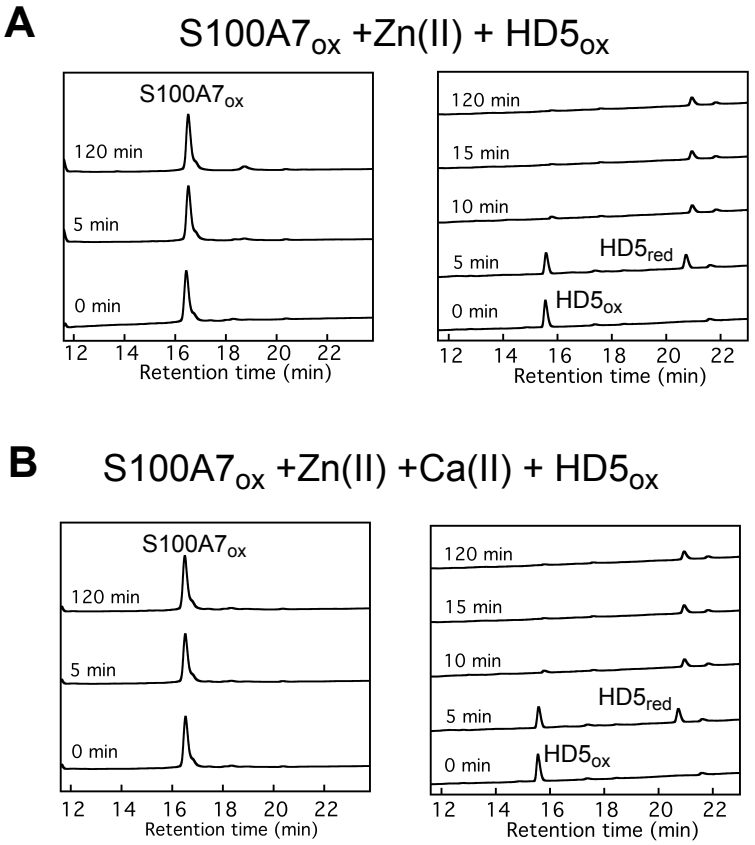

Figure S9. Analytical HPLC traces (220 nm) monitoring the reduction of $HD5_{ox}$ by Trx/TrxR in the presence of Zn(II)-bound $S100A7_{ox}$ in the (A) absence and (B) presence of 2 mM added Ca(II). (1 mM NADPH in 75 mM HEPES, 100 mM NaCl, pH 7.0). These assays served as controls for examining the effect of Zn(II)-$S100A7_{ox}$ on the activity of the thioredoxin system. Conditions: 10 μM $HD5_{ox}$, 5 μM $S100A7_{ox}$, 9.5 μM Zn(II), 1 μM human Trx, 0.1 μM rat liver TrxR, 1 mM NADPH, ±2 mM Ca(II).

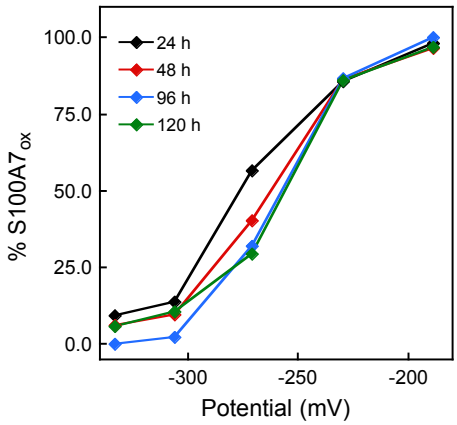

Figure S10. Percentage of $S100A7_{ox}$ at t = 24, 48, 96, and 120 h after incubation of 10 μM $S100A7_{ox}$ in glutathione-based redox buffers with defined redox potentials (75 mM HEPES, 100 mM NaCl, pH 7.0), at 37 °C under anaerobic conditions.

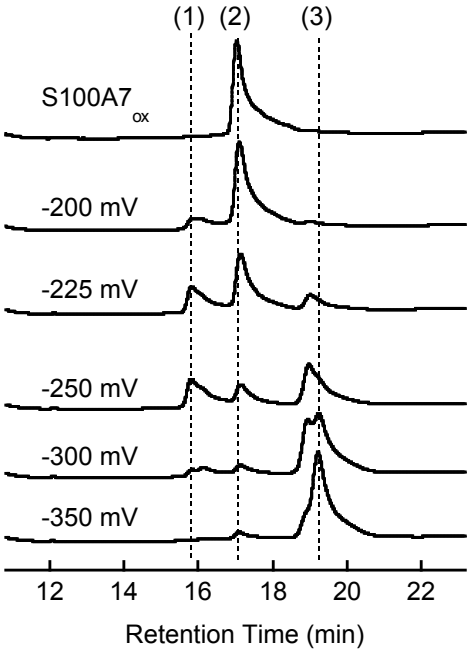

Figure S11. Representative HPLC traces showing the speciation of S100A7 after a 96-h incubation of 10 μM $S100A7_{ox}$ in glutathione-based redox buffers with defined redox potentials (75 mM HEPES, 100 mM NaCl, pH 7.0). Peak 1 corresponds to a glutathione-S100A7 mixed disulfide species, peak 2 corresponds to $S100A7_{ox}$, and peak 3 corresponds to $S100A7_{red}$. The identity of each peak was confirmed by LC-MS.

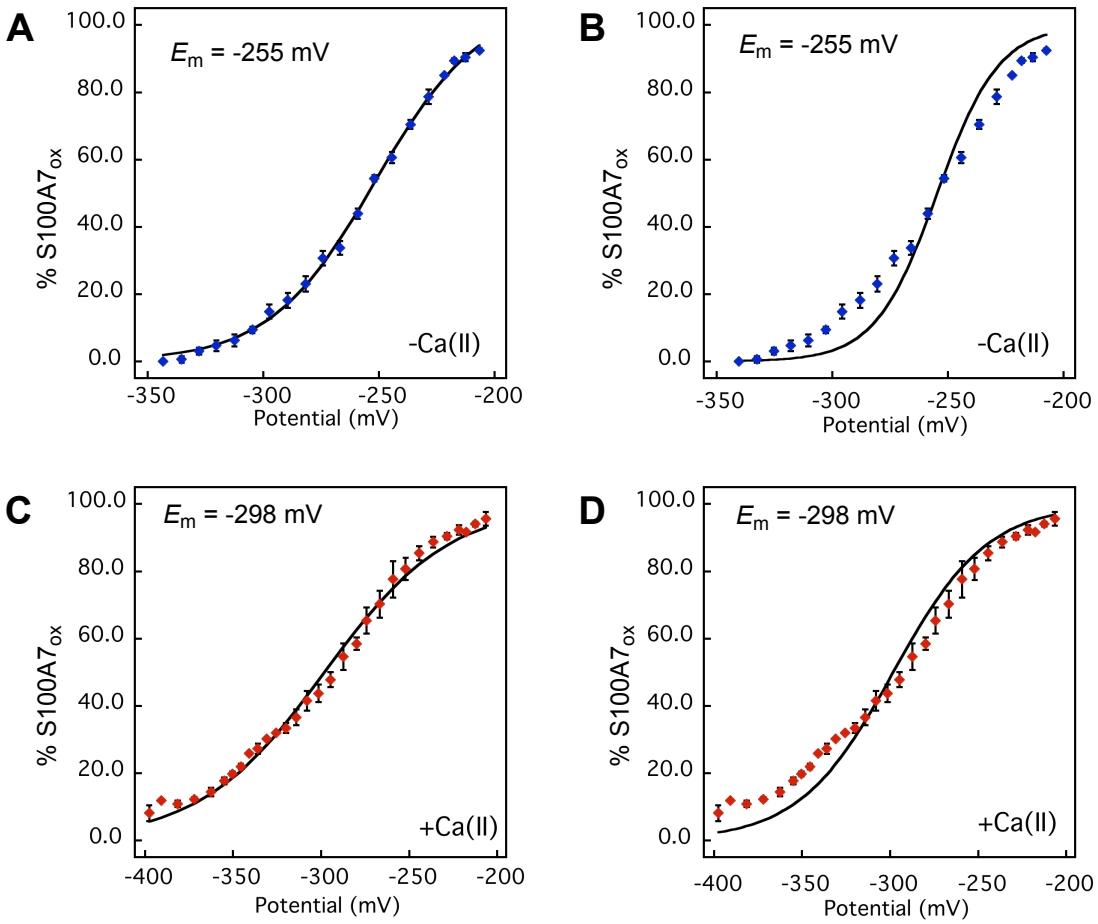

Figure S12. Midpoint potential data presented in Figure 4 were fit to a logistic function (A andC) and the Nernst equation (B and D). This experiment was performed in the absence (A and B, blue markers) and in the presence of 2 mM Ca(II) (C and D, red markers). Derivations for the Nernst and logistic functions are presented on pages S12 and S13, respectively.

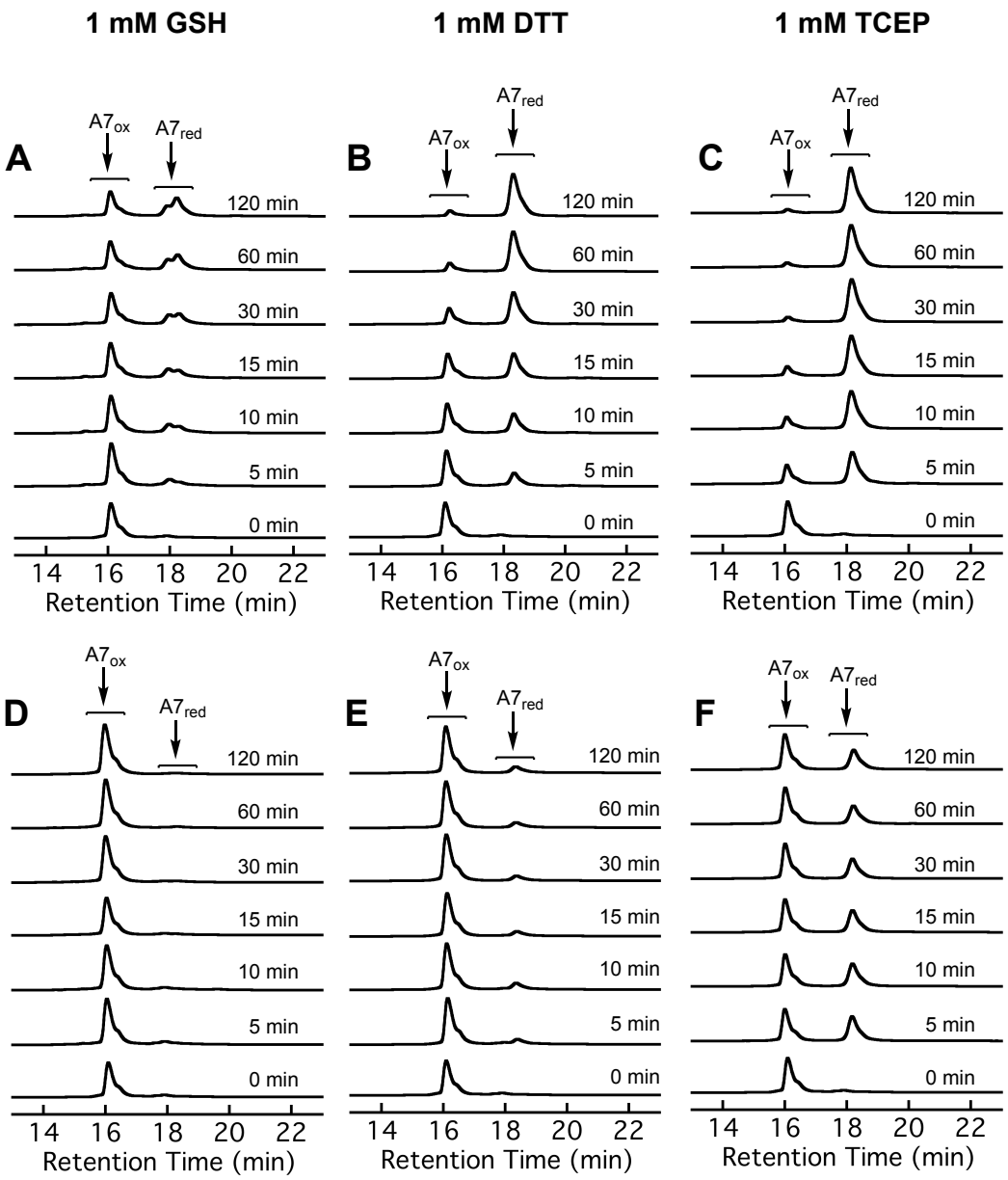

Figure S13. Representative HPLC traces showing the reduction of 30 μM $S100A7_{ox}$ to $S100A7_{red}$ in the absence (A-C) and presence (D-F) of Zn(II) following addition of 1 mM GSH, DTT or TCEP (75 mM HEPES, 100 mM NaCl, pH 7.0, room temperature, aerobic). For the Zn(II)-bound samples (D-F), $S100A7_{ox}$ was pre-incubated with 2 equivalents of Zn(II) (60 μM) for 15 min at room temperature prior to addition of the reducing agent.

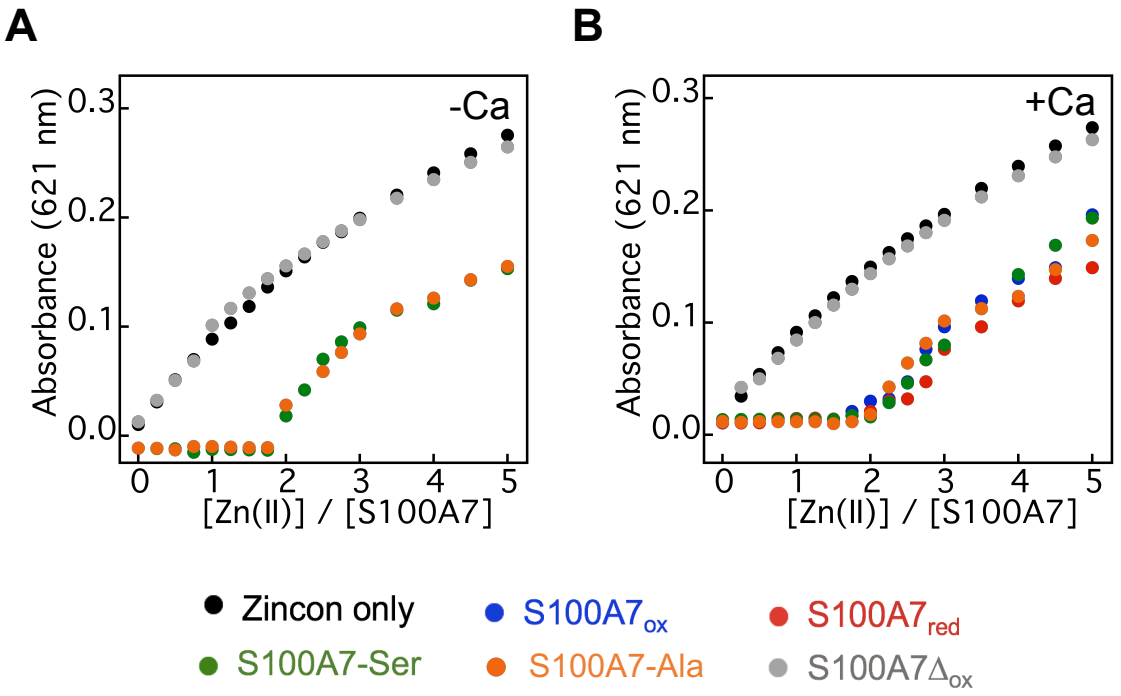

Figure S14. Representative plot showing the response of 20 μM Zincon to Zn(II) in the presence of 10 μM S100A7 proteins in 75 mM HEPES, 100 mM NaCl, pH 7.0, ±2 mM Ca(II) at 25 °C. (A) In the absence of Ca(II). Data for $S100A7_{red}$ and $S100A7_{ox}$ are shown in Figure 5 of the main text. (B) In the presence of Ca(II). The Zn(II)-Zincon complex exhibits an absorbance maximum at 621 nm.

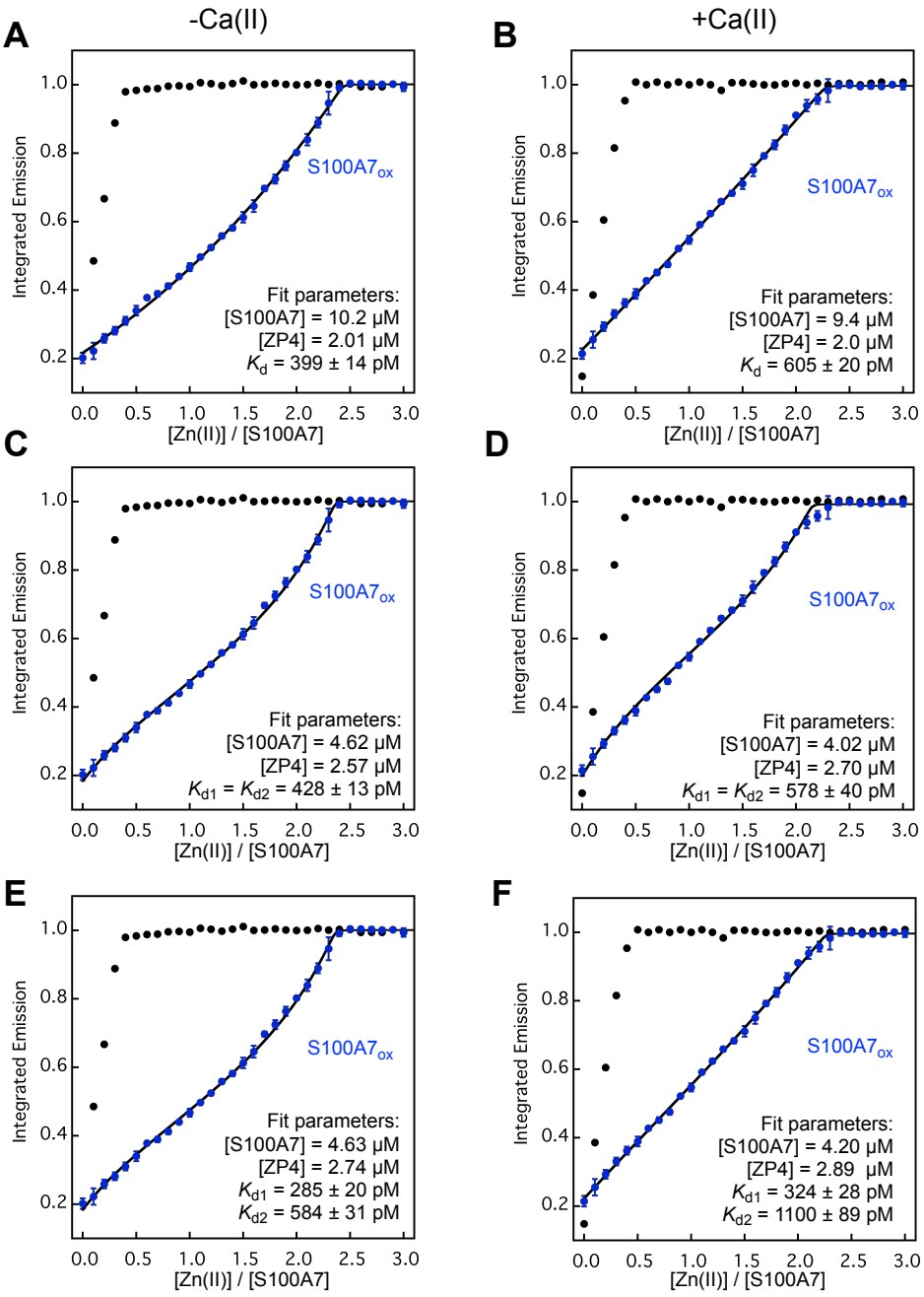

Figure S15. Zn(II)-induced response of 2 μM ZP4 in the presence of 5 μM S100A7$_{ox}$ at pH 7.0 (75 mM HEPES, 100 mM NaCl) at 25 °C, in the absence (left panels) and presence (right panels) of 100 equiv of Ca(II). The integrated emission was normalized to the maximum response (mean ± SDM, n = 3). The data were fit to a one-site binding model (A and B), two-sites binding model with $K_{d1} = K_{d2}$ (C and D), or a two-sites binding model with $K_{d1} \neq K_{d2}$ (E and F). In each panel, the black and blue spheres correspond to the ZP4 only control and the ZP4 response in the presence of S100A7$_{ox}$, respectively. The calculated apparent K_d values corresponding to the fits and the fit parameters are listed in the bottom right of each plot.

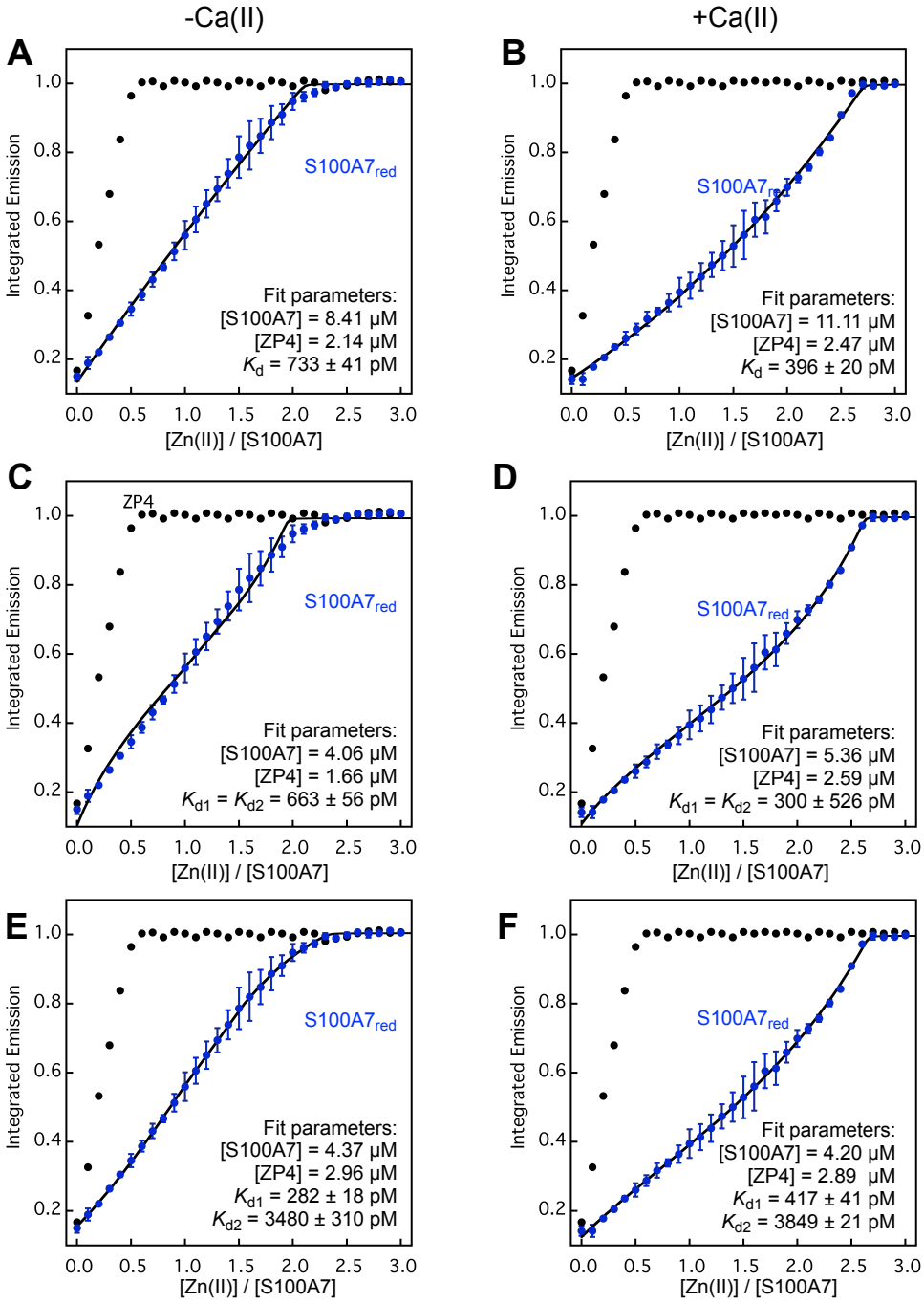

Figure S16. Zn(II)-induced response of 2 μM ZP4 in the presence of 5 μM S100A7$_{red}$ at pH 7.0 (75 mM HEPES, 100 mM NaCl) at 25 °C, in the absence (left panels) and presence (right panels) of 100 equiv of Ca(II). The integrated emission was normalized to the maximum response (mean ± SDM, n = 3). The data were fit to a one-site binding model (A and B), two-sites binding model with $K_{d1} = K_{d2}$ (C and D), or a two-sites binding model with $K_{d1} \neq K_{d2}$ (E and F). In each panel, the black and blue spheres correspond to the ZP4 only control and the ZP4 response in the presence of S100A7$_{red}$, respectively. The calculated apparent K_d values corresponding to the fits and the fit parameters are listed in the bottom right of each plot.

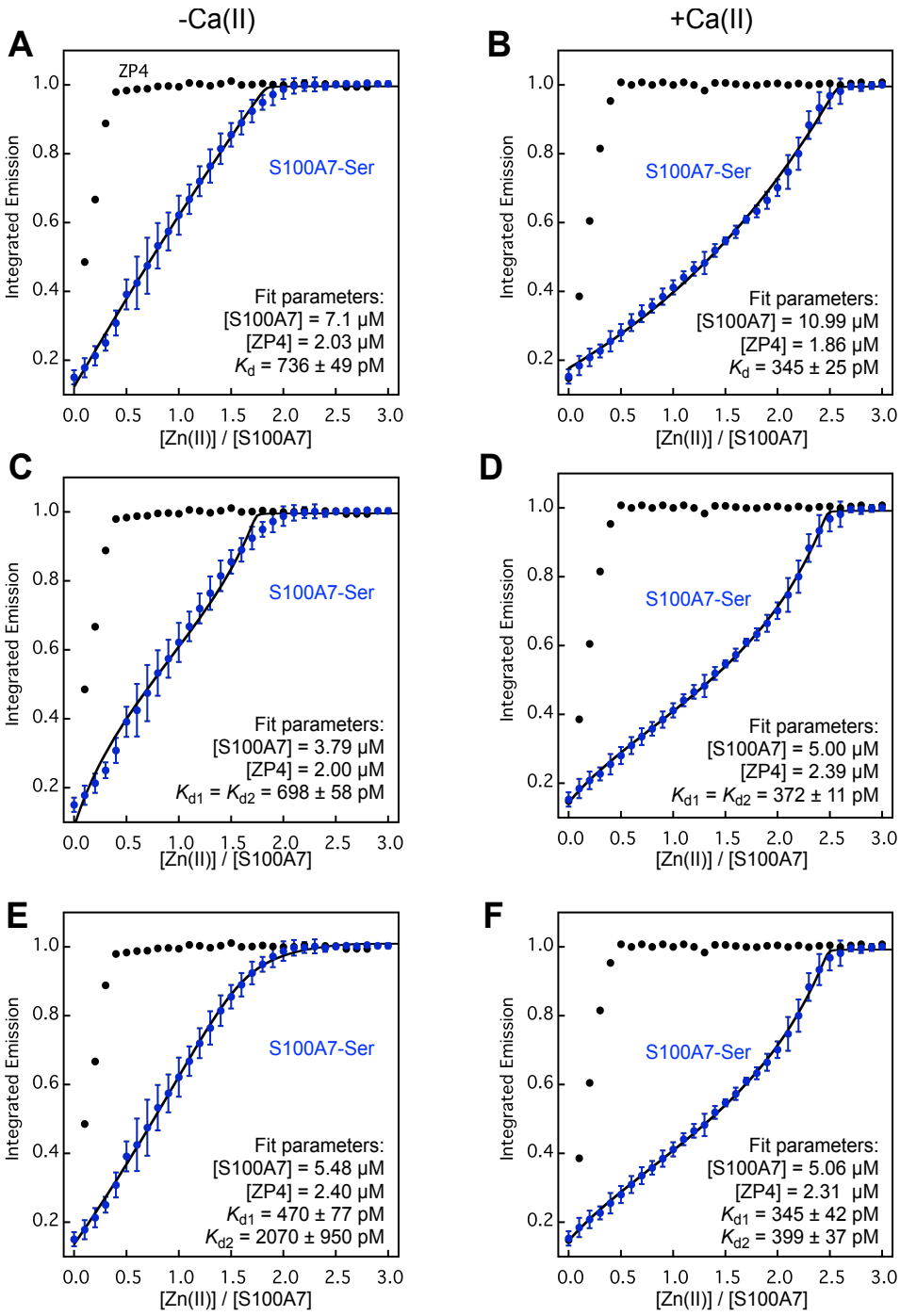

Figure S17. Zn(II)-induced response of 2 μM ZP4 in the presence of 5 μM S100A7-Ser at pH 7.0 (75 mM HEPES, 100 mM NaCl) at 25 °C, in the absence (left panels) and presence (right panels) of 100 equiv of Ca(II). The integrated emission was normalized to the maximum response (mean ± SDM, n = 3). The data were fit to a one-site binding model (A and B), two-sites binding model with $K_{d1} = K_{d2}$ (C and D), or a two-sites binding model with $K_{d1} \neq K_{d2}$ (E and F). In each panel, the black and blue spheres correspond to the ZP4 only control and the ZP4 response in the presence of S100A7-Ser, respectively. The calculated apparent K_d values corresponding to the fits and the optimized parameters are listed in the bottom right of each plot.

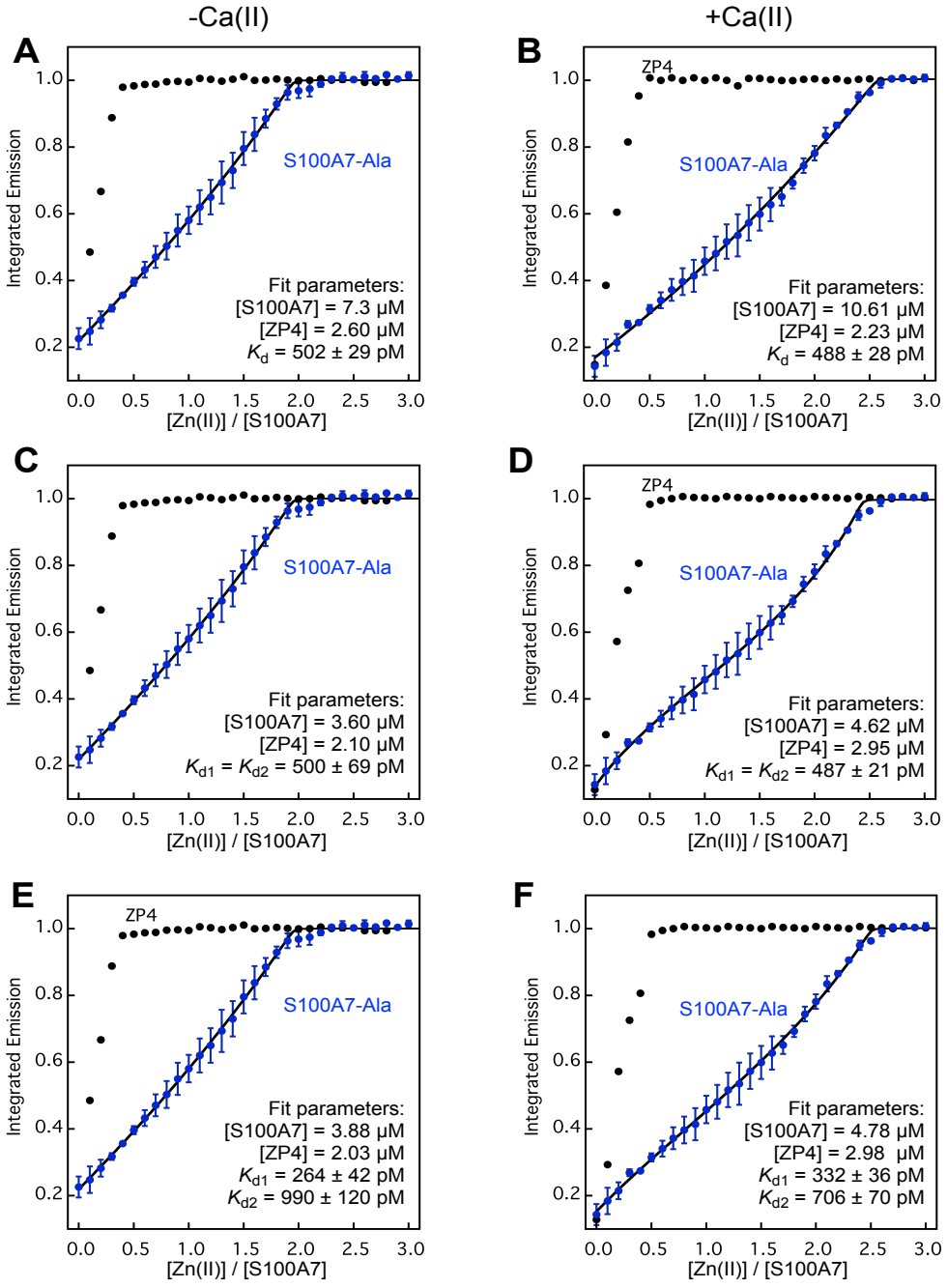

Figure S18. Zn(II)-induced response of 2 μM ZP4 in the presence of 5 μM S100A7-Ala at pH 7.0 (75 mM HEPES, 100 mM NaCl) at 25 °C, in the absence (left panels) and presence (right panels) of 100 equiv of Ca(II). The integrated emission was normalized to the maximum response (mean ± SDM, n = 3). The data were fit to a one-site binding model (A and B), two-sites binding model with K_{d1} = K_{d2} (C and D), or a two-sites binding model with $K_{d1} \neq K_{d2}$ (E and F). In each panel, the black and blue spheres correspond to the ZP4 only control and the ZP4 response in the presence of S100A7-Ala, respectively. The calculated apparent K_d values corresponding to the fits and the fit parameters are listed in the bottom right of each plot.

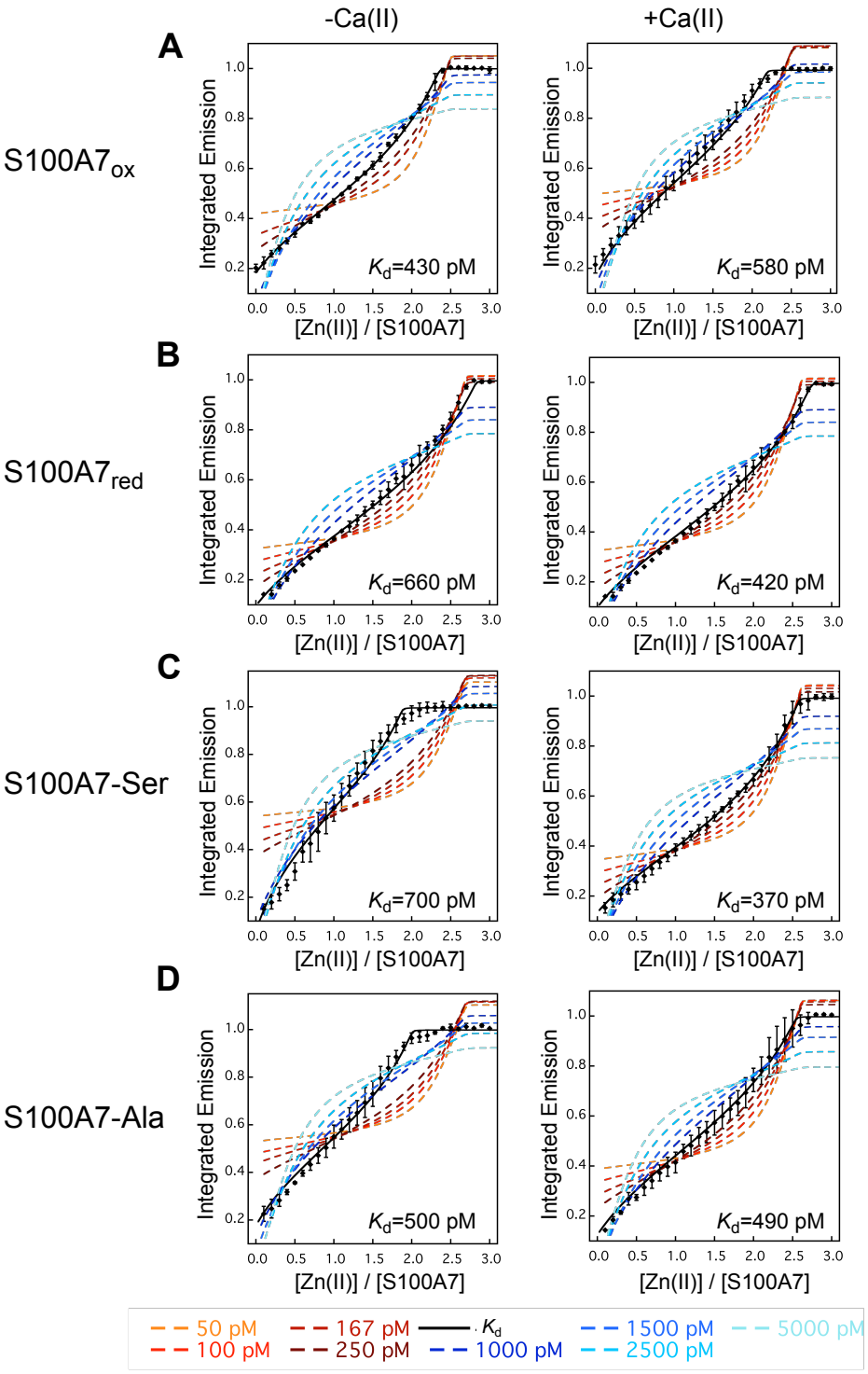

Figure S19 Simulated Zn(II) competition curves for ZP4 and (A) $S100A7_{ox}$, (B) $S100A7_{red}$, (C) S100A7-Ser, and (D) S100A7-Ala in the absence and presence of 100 equiv Ca(II). Curves were simulated employing K_d values from 50 to 5000 pM. The data were fit to a two-sites binding model with $K_{d1} = K_{d2}$. For all plots, the data are the black circles (mean ± SDM), and the reported fit is the black line. The colored dashed lines indicate the simulated curves.

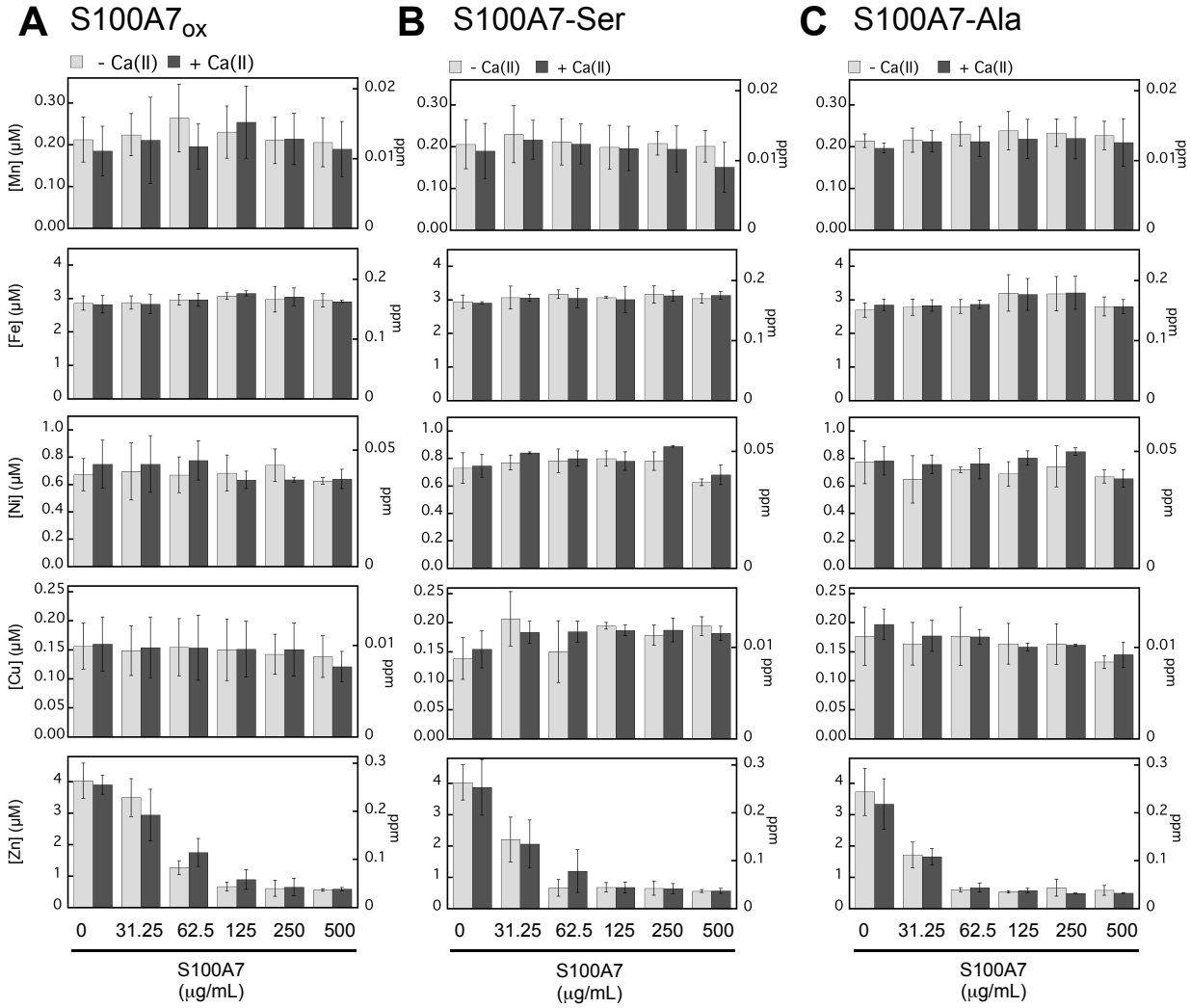

Figure S20. Metal analysis (Mn, Fe, Ni, Cu, Zn) of TSB:Tris medium treated with 0–500 μg/mL (A) $S100A7_{ox}$, (B) S100A7-Ser, and (C) S100A7-Ala. The experiments were conducted in the absence (light gray bars) and presence (dark gray bars) of a 2 mM Ca(II) supplement (mean ± SDM, *n* = 3).

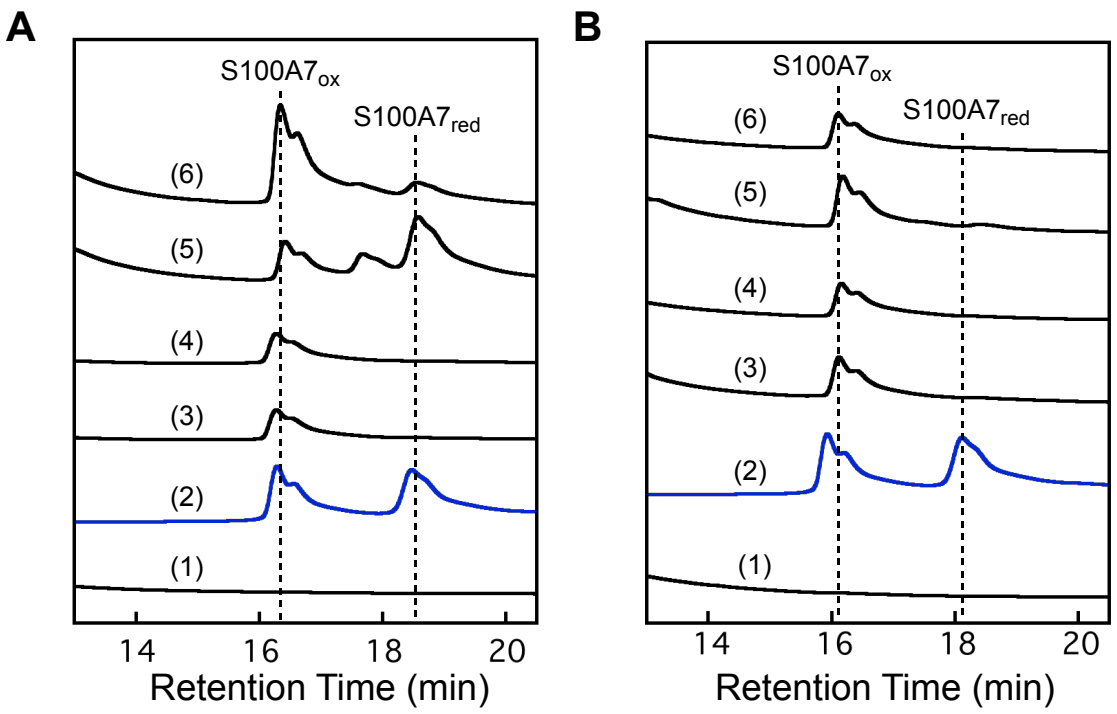

Figure S21. Speciation of S100A7 after incubating a ≈1:1 mixture (125 μg/mL) of $S100A7_{red}$ and $S100A7_{ox}$ for 20 h at 37 °C in (A) TSB:Tris medium without bacteria and (B) TSB:Tris medium with *E. coli* K-12. Trace (1) is Tris:TSB medium only, trace (2) is the S100A7 mixture in AMA buffer (20 mM Tris, 100 mM NaCl, pH 7.5) that serves as a standard, trace (3) is S100A7 after 20 h at 37 °C, trace (4) is S100A7 after 20 h at 37 °C in medium supplemented with 2 mM Ca(II), trace (5) is S100A7 after 20 h at 37 °C in medium supplemented with 5 mM β-mercaptoethanol, trace (6) is S100A7 after 20 h at 37 °C in medium supplemented with 2 mM Ca(II) and 5 mM β-mercaptoethanol.

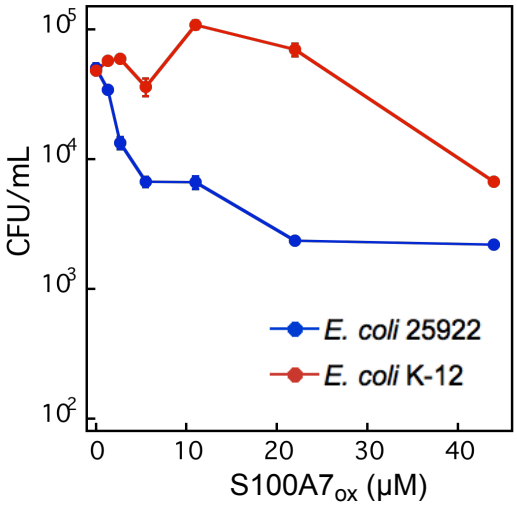

Figure S22. Microdilution antimicrobial activity assay of $S100A7_{ox}$ and *E. coli*. *E. coli* ATCC 25922 (blue) and *E. coli* K-12 (red) are killed by $S100A7_{ox}$ under these assay conditions (3 h, 37 ^{o}C, 150 rpm; 10 mM phosphate buffer pH 7.4 supplemented with 1% TSB).

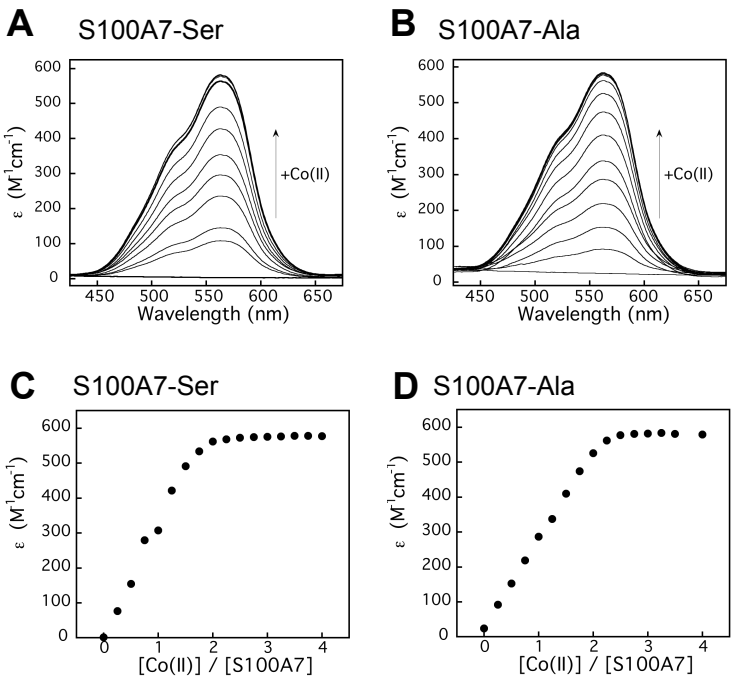

Figure S23. Co(II)-binding titrations with S100A7-Ser and S100A7-Ala. Optical absorption spectra titrations (top row) and ε_{563} versus equivalents of Co(II) added (bottom row) to 300 μM of S100A7-Ser (A and C), and S100A7-Ala (B and D) in 75 mM HEPES, 100 mM NaCl, pH 7.0 and 25 ^{o}C.

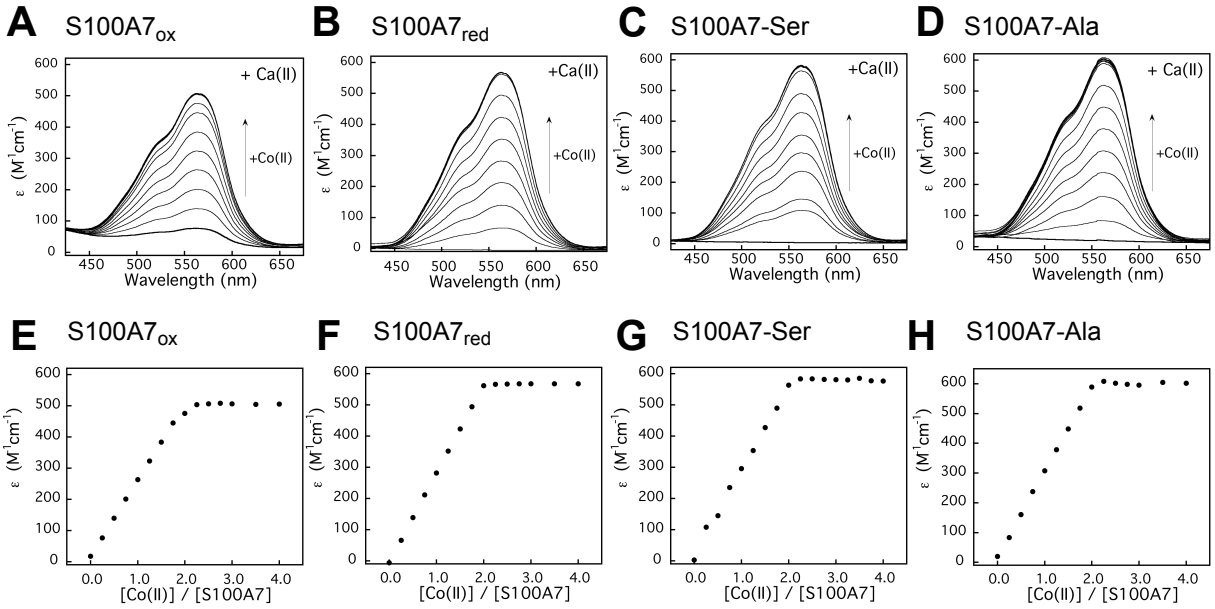

Figure S24. Optical absorption spectra (top row) and plots of ε_{563} versus equivalents of Co(II) added (bottom row) corresponding to titration of 300 μM of $S100A7_{ox}$ (A and E), $S100A7_{red}$ (B and F), S100A7-Ser (C and G), and S100A7-Ala (D and H) with 0–4 equivalents of Co(II) in 75 mM HEPES, 100 mM NaCl, 300 mM Ca(II), pH 7.0, and 25 ^{o}C.

Supporting References

[1] Brophy, M. B., Nakashige, T. G., Gaillard, A., and Nolan, E. M. (2013) Contributions of the S100A9 C-terminal tail to high-affinity Mn(II) chelation by the host-defense protein human calprotectin, *J. Am. Chem. Soc. 135*, 17804-17817.

[2] Wanniarachchi, Y. A., Kaczmarek, P., Wan, A., and Nolan, E. M. (2011) Human defensin 5 disulfide array mutants: disulfide bond deletion attenuates antibacterial activity against *Staphylococcus aureus*, *Biochemistry 50*, 8005-8017.

[3] Holmgren, A. (1985) Thioredoxin, *Ann. Rev. Biochem. 54*, 237-271.

[4] Zhang, Y. F., Cougnon, F. B. L., Wanniarachchi, Y. A., Hayden, J. A., and Nolan, E. M. (2013) Reduction of human defensin 5 affords a high-affinity zinc-chelating peptide, *ACS Chem. Biol. 8*, 1907-1911.

[5] Schafer, F. Q., and Buettner, G. R. (2001) Redox environment of the cell as viewed through the redox state of the glutathione disulfide/glutathione couple, *Free Radic. Biol. Med. 30*, 1191-1212.

[6] Burdette, S. C., Frederickson, C. J., Bu, W. M., and Lippard, S. J. (2003) ZP4, an improved neuronal Z^{n2+} sensor of the Zinpyr family, *J. Am. Chem. Soc. 125*, 1778-1787.

[7] Brophy, M. B., Hayden, J. A., and Nolan, E. M. (2012) Calcium ion gradients modulate the zinc affinity and antibacterial activity of human calprotectin, *J. Am. Chem. Soc. 134*, 18089-18100.

[8] Cunden, L. S., Gaillard, A., and Nolan, E. M. (2016) Calcium ions tune the zinc-sequestering properties and antimicrobial activity of human S100A12, *Chemical Science 7*, 1338-1348.

[9] Gläser, R., Harder, J., Lange, H., Bartels, J., Christophers, E., and Schröder, J. M. (2005) Antimicrobial psoriasin (S100A7) protects human skin from *Escherichia coli* infection, *Nat. Immunol. 6*, 57-64.

[10] Baba, T., Ara, T., Hasegawa, M., Takai, Y., Okumura, Y., Baba, M., Datsenko, K. A., Tomita, M., Wanner, B. L., and Mori, H. (2006) Construction of *Escherichia coli* K-12 in-frame, single-gene knockout mutants: the Keio collection, *Mol. Syst. Biol. 2*, 2006 0008.